Cellular/Molecular

Stabilization of $GABA_A$ Receptors at Endocytic Zones Is Mediated by an AP2 Binding Motif within the $GABA_A$ Receptor β3 Subunit

Katharine R. Smith,[1]* James Muir,[1,2]* Yijian Rao,[3] Marietta Browarski,[1] Marielle C. Gruenig,[3] David F. Sheehan,[1,2] Volker Haucke,[3] and Josef T. Kittler[1]

[1]Department of Neuroscience, Physiology, and Pharmacology and [2]Centre for Mathematics and Physics in the Life Sciences and Experimental Biology, University College London, London WC1E 6BT, United Kingdom, and [3]Freie Universität Berlin, 14195 Berlin, Germany

The strength of synaptic inhibition can be controlled by the stability and endocytosis of surface and synaptic $GABA_A$ receptors ($GABA_A$Rs), but the surface receptor dynamics that underpin $GABA_A$R recruitment to dendritic endocytic zones (EZs) have not been investigated. Stabilization of $GABA_A$Rs at EZs is likely to be regulated by receptor interactions with the clathrin-adaptor AP2, but the molecular determinants of these associations remain poorly understood. Moreover, although surface $GABA_A$R downmodulation plays a key role in pathological disinhibition in conditions such as ischemia and epilepsy, whether this occurs in an AP2-dependent manner also remains unclear. Here we report the characterization of a novel motif containing three arginine residues (^{405}RRR^{407}) within the $GABA_A$R β3-subunit intracellular domain (ICD), responsible for the interaction with AP2 and $GABA_A$R internalization. When this motif is disrupted, binding to AP2 is abolished *in vitro* and in rat brain. Using single-particle tracking, we reveal that surface β3-subunit-containing $GABA_A$Rs exhibit highly confined behavior at EZs, which is dependent on AP2 interactions via this motif. Reduced stabilization of mutant $GABA_A$Rs at EZs correlates with their reduced endocytosis and increased steady-state levels at synapses. By imaging wild-type or mutant super-ecliptic pHluorin-tagged $GABA_A$Rs in neurons, we also show that, under conditions of oxygen–glucose deprivation to mimic cerebral ischemia, $GABA_A$Rs are depleted from synapses in dendrites, depending on the ^{405}RRR^{407} motif. Thus, AP2 binding to an RRR motif in the $GABA_A$R β3-subunit ICD regulates $GABA_A$R residency time at EZs, steady-state synaptic receptor levels, and pathological loss of $GABA_A$Rs from synapses during simulated ischemia.

Introduction

$GABA_A$ receptors ($GABA_A$Rs) are the main mediators of inhibitory neurotransmission in the CNS and play an essential role in maintaining the excitatory/inhibitory balance required for correct brain function (Smith and Kittler, 2010). Modulating the abundance of $GABA_A$Rs at synaptic sites is a key mechanism for determining the strength of synaptic inhibition (Arancibia-Cárcamo and Kittler, 2009). However, the exact molecular processes that underlie changes in $GABA_A$R numbers at synapses and hence synaptic efficacy under normal or pathological conditions remain poorly understood.

$GABA_A$Rs are dynamic entities, in terms of both their lateral mobility at the plasma membrane (Bannai et al., 2009; Muir et al., 2010) and their trafficking to and from the cell surface (Smith and Kittler, 2010). Clathrin-mediated endocytosis of $GABA_A$Rs is dependent on the clathrin-adaptor AP2 and rapidly modulates synaptic $GABA_A$R number, inhibitory synaptic strength, neuronal excitability, and, ultimately, animal behavior (Kittler et al., 2000, 2005; Chen et al., 2006; Kurotani et al., 2008; Tretter et al., 2009). Although a number of recent studies have investigated the diffusion of $GABA_A$Rs into and out of synapses, far less is known about $GABA_A$R membrane dynamics at endocytic zones (EZs) and how $GABA_A$Rs are recruited to and stabilized at these regions.

Disrupted $GABA_A$R trafficking contributes to altered information processing in pathological conditions such as epilepsy and ischemia, in which acute receptor surface downmodulation and loss of synaptic $GABA_A$Rs leads to compromised neuronal inhibition and altered excitability states, but the underlying mechanisms remain unclear (Mielke and Wang, 2005; Naylor et al., 2005; Tan et al., 2007; Arancibia-Cárcamo et al., 2009). Indeed, although both clathrin-dependent and -independent (e.g., caveolar-dependent) pathways for $GABA_A$R endocytosis have been described (Kittler et al., 2000; Bradley et al., 2008), the specific contribution of AP2-dependent pathways for synaptic receptor loss in epilepsy or ischemia remains unclear. Deciphering the molecular mechanisms and endocytic pathways responsible for synaptic $GABA_A$R downmodulation is therefore central to understanding how synaptic inhibition is regulated in the healthy brain and could lead to identification of potential target pathways

Received March 29, 2011; revised Nov. 17, 2011; accepted Nov. 25, 2011.

Author contributions: K.R.S., J.M., and J.T.K. designed research; K.R.S., J.M., Y.R., M.B., M.C.G., D.F.S., V.H., and J.T.K. performed research; K.R.S. contributed unpublished reagents/analytic tools; K.R.S., J.M., Y.R., D.F.S., and V.H. analyzed data; K.R.S. and J.T.K. wrote the paper.

This work was supported by the United Kingdom Medical Research Council (J.T.K.) and by the German funding agency Deutsche Forschungsgemeinschaft [Exc-257, HA2686/3-2 (FG806) (V.H.)]. J.M. and D.F.S. are in the CoMPLEX PhD Programme at University College London. We thank David Attwell for the use of his confocal microscope.

*K.R.S. and J.M. contributed equally to this work.

Correspondence should be addressed to Dr. Josef Kittler, Department of Neuroscience, Physiology, and Pharmacology, University College London, Gower Street, London WC1E 6BT, UK. E-mail: j.kittler@ucl.ac.uk.

DOI:10.1523/JNEUROSCI.1622-11.2011

 0270-6474/12/322485-14$15.00/0

of pathological receptor downmodulation for therapeutic intervention during disinhibition in disease.

Here, we characterize the molecular interactions that underlie internalization of $GABA_A$Rs containing β3 subunits, which are present in a large proportion of receptor subtypes in the hippocampus and cortex, regions that are particularly vulnerable to excitotoxicity (Lo et al., 2003). Using a combination of molecular, biochemical, and imaging approaches, we identify a three arginine (RRR) motif within the $GABA_A$R β3-subunit intracellular domain (ICD) that mediates the clathrin-dependent endocytosis of $GABA_A$Rs via direct binding to AP2. Furthermore, by combining single-particle tracking with mutagenesis of the RRR motif, we reveal that $GABA_A$Rs are reversibly stabilized at EZs, depending on interactions with AP2. Additionally, we demonstrate that loss of synaptic $GABA_A$Rs in an *in vitro* model of ischemia is dependent on AP2-binding via this motif and that blocking this mechanism can reduce cell death. Thus, direct binding of $GABA_A$R ICDs to AP2 regulates $GABA_A$R recruitment into EZs, steady-state $GABA_A$R levels at synapses, and provides a key mechanism for receptor downmodulation in pathology.

Materials and Methods

cDNA cloning. The β3 $GABA_A$R-subunit mutants were made by site-directed mutagenesis on a pRK5$^{myc}\beta$3 backbone. The ICDs of these mutants were amplified by PCR, and the resulting fragment was inserted into the BamH1/Not1 sites of pGEX–4T3. $^{SEP}\gamma$2 (Superecliptic pHluorin) has been described previously (Muir et al., 2010). Untagged α1 was in pRK5 and was described previously (Twelvetrees et al., 2010). mRFP–rab5 [Addgene plasmid 14437 (Vonderheit and Helenius, 2005)] and clathrin-light chain polypeptide–EYFP [Addgene plasmid 21741 (Chen and Zhuang, 2008)] were from Addgene. EGFP was from Clontech.

Antibodies. The following primary antibodies were used: mouse monoclonal anti-Myc was obtained from 9E10 hybridoma cells [immunofluorescence (IF) and ELISA, supernatant 1:100], anti-AP50 [Western blot (WB), 1:250; BD Biosciences], anti-GFP (IF, 1:500; clone N86/38; Neuromab), rabbit polyclonal anti-myc [IF, 1:200; quantum dot (QD) imaging, 1:100; Santa Cruz Biotechnology], rabbit anti-vesicular inhibitory amino acid transporter (VIAAT) [a kind gift from B. Gasnier, Universite Paris, Descartes, France (Dumoulin et al., 1999); IF, 1:1000], anti-α1 $GABA_A$R subunit (WB, 1:5; clone N95/35; Neuromab), anti-β-adaptin (WB, 1:500; Sigma), vesicular GABA transporter (VGAT)–Oyster 488 (live imaging, 1:1000; Synaptic Systems), and anti-myc (QD imaging, 1:100; Millipore Bioscience Research Reagents).

Cell culture. Cultures of cortical and hippocampal neurons were prepared from E18 Sprague Dawley rat embryos of either sex as described previously (Kittler et al., 2004). Neurons were transfected by nucleofection before plating as described previously (Kittler et al., 2004; Macaskill et al., 2009; Twelvetrees et al., 2010). COS-7 cells were maintained in DMEM (Invitrogen), supplemented with 10% heat-inactivated fetal bovine serum and penicillin–streptomycin, and transfected by electroporation (Kittler et al., 2004) for biochemistry and by nucleofection (Amaxa) for immunocytochemistry.

GST fusion protein pull-down assays from rat brain homogenate. Pull-downs from brain were performed as described previously (Smith et al., 2008, 2010). Briefly, adult rat brain was homogenized in pull-down buffer (50 mM HEPES, pH 7.5, 0.5% Triton X-100, 150 mM NaCl, 1 mM EDTA, and 1 mM PMSF with antipain, pepstatin, and leupeptin at 10 μg/ml) and solubilized for 2 h. Solubilized material was ultracentrifuged at 66,000 × *g* for 40 min at 4°C, and the supernatant (solubilized protein) was exposed to 10–20 μg of GST fusion protein attached to glutathione–agarose beads for 1 h at 4°C. Beads were then washed extensively and analyzed by SDS-PAGE and WB.

In vitro *translation of [^{35}S]methionine-labeled protein and GST pull-down assays.* Residues 156–433 of the μ2 subunit of AP2 were *in vitro* translated using TNT SP6 Quick Coupled Transcription/Translation system (Promega) and labeled with [^{35}S]methionine (GE Healthcare) following the protocol of the manufacturer (Smith et al., 2008, 2010). Five microliters of labeled protein were incubated with 10–20 μg of GST fusion protein in pull-down buffer (as above) for 2 h at 4°C. The beads were washed and resolved by SDS-PAGE followed by staining with Coomassie blue. Radioactivity was detected with a phosphor-storage screen and PhosphorImager. Bacterially expressed wild-type (WT) or mutant (mut) His-tagged μ2 were used for nonradioactive *in vitro* pull-downs with GST fusion proteins and analyzed by SDS-PAGE, followed by staining with Coomassie blue (Smith et al., 2008).

Surface plasmon resonance. Surface plasmon resonance (SPR) experiments were performed as described previously (Kittler et al., 2008) on a BIAcore 2000 instrument (BIAcore).

Immunofluorescence. For receptor internalization assays in COS-7 cells, receptors were live labeled with 9E10 anti-myc antibody in HEPES buffer (in mM: 25 HEPES, 140 NaCl, 5.4 KCl, 1.8 $CaCl_2$, and 15 glucose, pH 7.4) at 4°C. Labeled receptors were allowed to internalize for 30 min at 37°C, and surface antibody was stripped away using 0.2 M acetic acid and 0.5 M NaCl before fixation as described previously (Arancibia-Cárcamo et al., 2009). Internalized receptors were identified using Alexa Fluor-594-conjugated or Alexa Fluor-488-conjugated anti-mouse secondary antibody (1:1000; Invitrogen) and confocal microscopy. Quantification of receptor internalization was performed by determining the area of the internalized receptors and normalization to the cell area (as given by GFP fluorescence; described by Hanley and Henley, 2005) or by measuring the colocalization of the internalized receptors with the early endosomal marker rab5.

Receptor internalization assays in neurons were performed similarly to what has been described previously (Scott et al., 2004), with modifications. Briefly, transfected neurons were incubated at room temperature with anti-9E10 antibody and placed at 37°C for 30 min to enable internalization. After washing, cells were fixed and surface receptors were stained with secondary Alexa Fluor-488 secondary antibody. Cells were permeabilized and stained with Alexa Fluor-594 secondary antibody to label the total receptor population and then visualized by confocal microscopy. For quantification of receptor internalization, red fluorescence that was not colocalized with green fluorescence (surface receptors) was calculated as the internalized receptor population and normalized to total receptor population.

Neurons for surface staining were fixed with 4% paraformaldehyde (PFA)/4% sucrose/PBS, pH 7, for 4 min and blocked with block solution (PBS, 10% horse serum, and 0.5% BSA) for 10 min. Neurons were incubated for 1 h with anti-9E10, followed by permeabilization with block solution containing 0.2% Triton X-100. Neurons were then incubated with anti-VIAAT antibody and subsequently with Alexa Fluor-488 and Alexa Fluor-594 secondary antibodies (1:1000; Invitrogen). After extensive washing, coverslips were mounted on microscope slides using ProLong Gold antifade reagent (Invitrogen) and sealed with nail varnish. Images were acquired using a Carl Zeiss Pascal confocal microscope and digitally captured using LSM software.

Surface receptor ELISA assay. Quantification of surface myc-tagged $GABA_A$Rs was performed by colorimetric cell ELISA as described previously (Mielke and Wang, 2005). Briefly, 8–9 DIV cultured cortical neurons were fixed with 4% PFA/sucrose for 5 min and then blocked under nonpermeabilizing conditions (PBS and 3% BSA). Cells were incubated for 1 h with anti-9E10 (1:100) and then for 1 h with HRP-conjugated anti-mouse secondary antibody (1:2000; Rockland). After extensive washing, cells were incubated with 1 vol of *o*-phenylenediamine substrate (Sigma) for 3 min. Reactions were stopped using 0.2 vol of 3N HCl, and 1 ml of supernatant was used to determine the absorbance at 492 nm. For *N*-ethylmaleimide-sensitive factor (NSF) inhibition experiments, COS-7 cells expressing myc-tagged $GABA_A$Rs were incubated with a TAT-fused NSF inhibitory peptide (NSFi) or scrambled control peptide for 75 min (Anachem) (Morrell et al., 2005; Chou et al., 2010), followed by the ELISA procedure described above.

Live-cell imaging and oxygen–glucose deprivation. Hippocampal neurons were nucleofected at time of plating with $^{myc}\beta$3 (WT, RRR/AAA or 7A), $^{SEP}\gamma$2, and untagged α1 in a ratio of 2:1:1. To assess the cotransfection of $^{myc}\beta3^{WT}$, $^{myc}\beta3^{RRR/AAA}$, and $^{myc}\beta3^{7A}$ with the $^{SEP}\gamma$2 in hippocampal neurons, neurons were live labeled for 15 min with a mouse anti-GFP antibody diluted in HEPES buffer (in mM: 25 HEPES, 140

NaCl, 5.4 KCl, 1.8 $CaCl_2$, and 15 glucose, pH 7.4) to label $^{SEP}\gamma2$ clusters. Cells were then fixed and blocked as described above and labeled with rabbit anti-myc antibody to label $^{myc}\beta3$-subunit-containing receptors. Coverslips were washed and mounted as described above. Quantification of cotransfection was performed by assessing whether the $^{SEP}\gamma2$-transfected neurons in a 40× field of view were also expressing $^{myc}\beta3$ subunits. This was then expressed as a percentage of the $^{SEP}\gamma2$-transfected neurons.

Cells were imaged at 12–15 DIV as described previously (Arancibia-Cárcamo et al., 2009). Carbonate-buffered solution contained 126 mM NaCl, 2.5 mM KCl, 1 mM $MgCl_2$, 2 mM $CaCl_2$, 1 mM NaH_2PO_4, 24 mM $NaHCO_3$, and 10 mM glucose and was gassed with 95% O_2, 5% CO_2. For oxygen–glucose deprivation (OGD), 7 mM sucrose was used in place of glucose, and the solution was gassed with 95% N_2, 5% CO_2. Both solutions were bubbled for 30 min before addition of $CaCl_2$ to prevent precipitate formation. Solutions were perfused at a constant rate of ~2 ml/min and heated to 35–37°C. For OGD experiments, the solution was switched from control to OGD buffer at $t = 0$ min. Super-ecliptic pHluorin fluorescence was captured using an Olympus microscope (BX51WI) with a 60× Olympus objective coupled to an EM-CCD camera (Ixon; Andor). Excitation was provided by a mercury-spiked xenon arc lamp (Cairn). Bandpass filters for excitation and emission were used (470/40 and 525/50 nm, respectively). Images (averages of eight consecutive exposures of 150 ms) were acquired every 10 min. The StackReg macro (Thévenaz et al., 1998) was used to correct for minor *x–y* drift that may have occurred between time points. Using NIH ImageJ, regions of interest were drawn around each non-somatic fluorescent cluster. After background subtraction, the average intensity across SEP-$GABA_A$R clusters in each time point was used as readout. This value was normalized to that at $t = 0$ min.

For cell death assays, hippocampal cultures were transduced with peptides (β3 peptide, KTHLRRRSSQLK; control peptide, INRVDAHENAAAAPM) for 1 h using Chariot reagent (active motif) following the instructions of the manufacturer (Kittler et al., 2008; Twelvetrees et al., 2010). After peptide transduction, cultures were exposed to 40 min OGD using a Billups-Rothenberg modular incubator chamber as described previously (Dixon et al., 2009) using the control and OGD buffers described above. To monitor cell death, 24 h after OGD treatment, neurons were stained with propidium iodide (PI) (4 μg/ml) for 1 h, followed by fixation with 4% PFA/sucrose and staining with DAPI. For each experiment, six to eight fields of view were imaged per condition, and the number of DAPI-positive nuclei that were PI stained was determined.

Single-particle tracking. Labeling of myc-tagged $GABA_A$Rs ($^{myc}\beta3^{WT}$ and $^{myc}\beta3^{RRR/AAA}$) with QDs was performed using a rabbit anti-myc antibody (Santa Cruz Biotechnology) or mouse anti-myc antibody (Millipore Bioscience Research Reagents) and anti-rabbit or anti-mouse 605 nm QDs (Invitrogen). Labeling was performed at room temperature with primary antibody (0.1 μg/ml, 1:100) for 8 min in block solution (imaging media containing 10% horse serum) and then QD incubation (0.5 nM) for 2 min in block solution as above. QD movies were recorded for 200 frames at 8.5 Hz (23.5 s duration). The imaging media for these experiments contained the following (in mM): 125 NaCl, 5 KCl, 1 $MgCl_2$, 2 $CaCl_2$, 10 D-glucose, and 10 HEPES, adjusted to pH 7.4. Labeling of inhibitory presynaptic terminals with VGAT–Oyster 488 (1:1000; Synaptic Systems) was performed by incubation of coverslips in 200 μl of imaging media for 30 min at 37°C, 5% CO_2, and we found that spontaneous activity in the neuronal culture was sufficient to load the dye into inhibitory presynaptic terminals. Similar staining could be achieved with a depolarizing high KCl stimulus (60 mM, 5 min; data not shown).

For analysis of single $GABA_A$R dynamics, trajectories were created automatically from movies of QD-tagged receptors. For each frame, an image segmentation algorithm was run that classifies image pixels based on their local symmetry at a specified scale. Pixels with maximal rotational symmetry (corresponding to local maxima in intensity) were classified as being attributable to QDs, and their locations were given to subpixel accuracy by taking the weighted average of connected target pixels. The pointing accuracy of the system is ~50 nm. Tracks were generated by linking particle positions between frames, using homemade software written in Mathematica (Wolfram Research). Briefly, the Euclidian distance between frames was minimized using a function that allowed for particle blinking such that tracks could be connected across blinking events. Instantaneous diffusivities (D_{inst}) were calculated from interframe displacements along consecutive track segments according to the 2D diffusion law ($x^2 = 4D_{inst}t$), and fitting to the first five points of the displacement curve was used to estimate the instantaneous diffusion coefficient. QD track segments were classified as being inside clathrin-coated pits (labeled by clathrin–YFP) if their midpoint was within 0.4 μm of the center of a pit. Cluster positions were found automatically from images taken immediately before the corresponding QD movie using the image segmentation algorithm described above. For imaging at inhibitory synapses, QD track segments were classified as synaptic if their midpoint was within 0.75 μm of the center of a VGAT punctum.

Statistical analysis. All experiments were performed at least three times from different preparations. Unless otherwise stated, *p* values given are from two-tailed *t* tests, and values are given as mean ± SEM. Error bars represent SEM.

Results

AP2 binds to a patch of basic amino acid residues within the β3-subunit ICD

Little is currently known regarding the dynamics of $GABA_A$Rs at EZs in neuronal dendrites for their subsequent endocytosis. Recruitment of $GABA_A$Rs to these sites is likely to depend on direct associations between the μ2 subunit of the clathrin adaptor AP2 (μ2–AP2) and $GABA_A$R-subunit ICDs (Kittler et al., 2005). To allow us to study the role of $GABA_A$R β3 subunits in regulating the dynamics of $GABA_A$R endocytosis, we set out to identify β3-subunit mutants no longer able to directly bind μ2–AP2. To this end, we made multiple GST fusion proteins of the β3-subunit ICD with sequential regions of the ICD deleted (Fig. 1*A*) and tested their ability to bind *in vitro* translated ^{35}S-labeled μ2–AP2. Quantification of the radioactive protein bound to the various GST–β3 ICD deletions revealed that the binding of μ2–AP2 to deletion 6 (Δ395–414) was significantly reduced compared with binding to the other GST–β3 ICD deletions ($n = 5$, $^*p < 0.05$; Fig. 1*B*,*C*). To ascertain whether a similar loss of binding was observed for μ2–AP2 from brain, we used a similar pull-down approach to assess the binding of GST–β3 deletion proteins to μ2–AP2 from rat brain homogenate. In agreement with our findings using radiolabeled μ2–AP2, the binding of brain μ2–AP2 to deletion 6 was significantly reduced compared with the other GST–β3 deletion proteins ($n = 4$, $^*p < 0.05$; Fig. 1*D*,*E*), further confirming that the region deleted in GST–β3 deletion 6 is important for the binding of μ2–AP2 to the β3-subunit ICD.

The 20 aa region identified in Figure 1*A–E* (deletion 6) contains a stretch of amino acids enriched with basic lysine and arginine residues, similar to motifs identified in other AP2-binding membrane proteins, including synaptotagmin-1 (Syt-1) (Haucke et al., 2000), the $\alpha1\beta$-adrenergic receptor (Diviani et al., 2003) and AMPA receptors (Kastning et al., 2007). To determine whether these residues within the β3 subunit (^{400}KKTHLRRR^{407}) were responsible for AP2 binding, we mutated the basic amino acids within this region to alanines (GST–$\beta3^{7A}$; Fig. 1*F*). A dileucine motif within the β2 $GABA_A$R-subunit ICD has also been suggested to be a determinant of clathrin-dependent internalization of the receptor (Herring et al., 2003). To verify whether a conserved dileucine motif in the β3-subunit ICD was also important for AP2 binding, we also mutated this motif to alanine (Fig. 1*F*), to give GST–$\beta3^{ILL/AAA}$, and additionally constructed a double mutant, GST–$\beta3^{7A+ILL/AAA}$ with both sites mutated. These fusion proteins were used in pull-down assays with ^{35}S-labeled μ2–AP2 to analyze the effect of these specific mutations on the AP2/β3 ICD interaction. Mutation of the seven basic res-

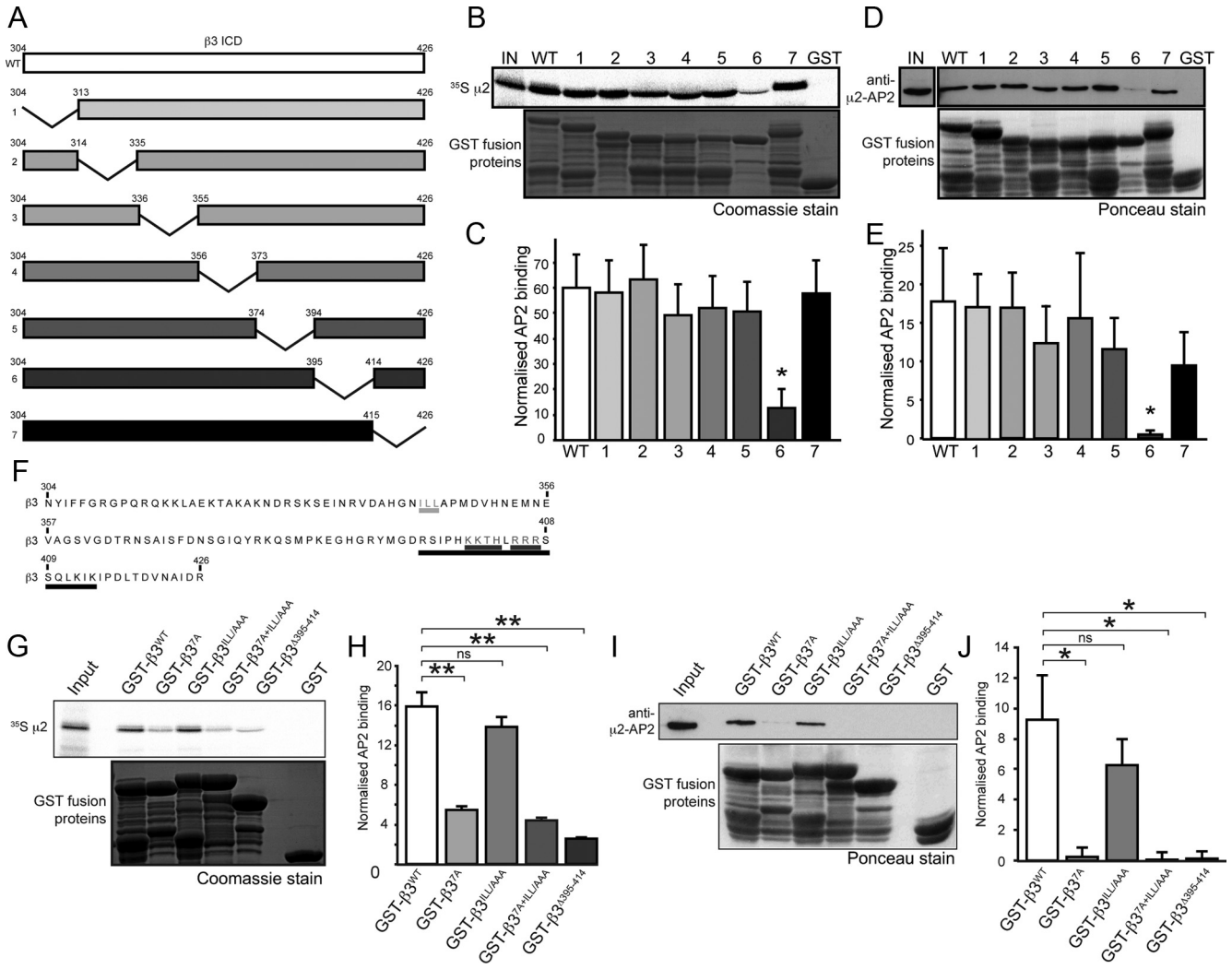

Figure 1. Identification of the interaction domain within the GABA$_A$R β3-subunit ICD that mediates association with AP2. ***A***, Schematic showing deletions within the GABA$_A$R β3-subunit ICD. ***B***, *In vitro* translated ^{35}S-labeled μ2 was subjected to pull-down experiments with deletion β3 ICD GST fusion proteins. IN, Input. ***C***, Quantification of μ2 binding shows a significant decrease in binding to deletion 6 (Δ395–414) ($n = 5$, $^*p < 0.05$). ***D***, Pull-down experiments with rat brain lysate with the deletion β3 ICD GST fusion proteins. Protein complexes were analyzed by SDS-PAGE and Western blotting with an antibody to AP2. ***E***, Densitometric quantification of endogenous AP2 binding to deletion β3 ICDs reveals a significant decrease in binding of AP2 to deletion 6 (Δ395–414) ($n = 4$, $^*p < 0.05$). ***F***, Amino acid sequence of the GABA$_A$R β3-subunit ICD. Deletion 6 (Δ395–414) is shown by the black line. Basic residues that may be a putative AP2 binding site are highlighted in dark gray and are mutated to alanine in the β3^{7A} mutant construct. A putative dileucine motif is highlighted in light gray. ***G***, *In vitro* translated ^{35}S-labeled μ2 was subjected to pull-down experiments with β3-subunit mutant GST fusion proteins. ***H***, Quantification of μ2 binding showing that the mutation of seven basic residues (β3^{7A}) within the region 395–414 significantly reduces binding of μ2 to the β3 ICD ($n = 3$, $^{**}p < 0.01$). ***I***, Pull-down experiments in rat brain lysate with the deletion β3-subunit mutant GST fusion proteins. Protein complexes were analyzed by SDS-PAGE and Western blotting with an antibody to AP2. ***J***, Quantification of endogenous AP2 binding to β3-subunit mutant ICDs showing the mutation of seven basic residues significantly reduces the binding of endogenous AP2 to the β3 ICD ($n = 6$, $^*p < 0.05$), but the mutation of the dileucine motif has no significant effect on AP2 binding.

idues greatly reduced binding of μ2–AP2 to the β3-subunit ICD by threefold ($n = 3$, $^{**}p < 0.01$; Fig. 1*G*,*H*), to a similar level to the binding of μ2–AP2 to β3 deletion 6 (β3$^{\Delta 395-414}$). However, the mutation of the dileucine motif to alanines had no significant effect on the binding of μ2–AP2 to the β3 ICD, and mutation of both motifs (β3$^{7A+ILL/AAA}$) had a similar effect to the 7A mutant alone, suggesting that the dileucine motif does not significantly contribute to the interaction with μ2–AP2. These experiments also corroborate the results from Figure 1*B–E*, which show no decrease in binding to AP2 with deletion 3, which contains the putative dileucine motif. Similar results were obtained from pull-down experiments with rat brain homogenate with binding of μ2–AP2 to the β3 ICD mutants mirroring the *in vitro* pull-down assays ($n = 6$, $^*p < 0.05$; Fig. 1*I*,*J*). These results support a key role for a 7 aa motif (^{400}KKTHLRRR^{407}) within the GABA$_A$R β3-subunit ICD in mediating the interaction with AP2.

Molecular determinants of the β3-subunit/AP2 interaction

To further identify the key residues within the ^{400}KKTHLRRR^{407} motif that mediate AP2 binding, we sequentially mutated the seven basic amino acids (shown in Fig. 2*A*) within GST–β3 ICD to alanine, generating GST–β3$^{KK/AA}$, GST–β3$^{TH/AA}$, and GST–β3$^{RRR/AAA}$ mutants, which were then used in pull-down experiments with rat brain homogenate (Fig. 2*B*). Quantification of AP2 binding by densitometry showed a large decrease in the binding of AP2 to the GST–β3$^{RRR/AAA}$ mutant compared with the binding to the GST–β3^{WT}, GST–β3$^{KK/AA}$, and GST–β3$^{TH/AA}$ fusion proteins ($n = 3$, $^*p < 0.05$; Fig. 2*C*), suggesting that these three arginine residues are essential for the binding of the β3 ICD to AP2. AP2 comprises a heteromer of α, β2, σ2, and μ2 adaptin subunits (Collins et al., 2002). We further confirmed that the RRR motif mediates interaction with heteromeric AP2 endogenous complexes as revealed by WB with a β2 adaptin antibody

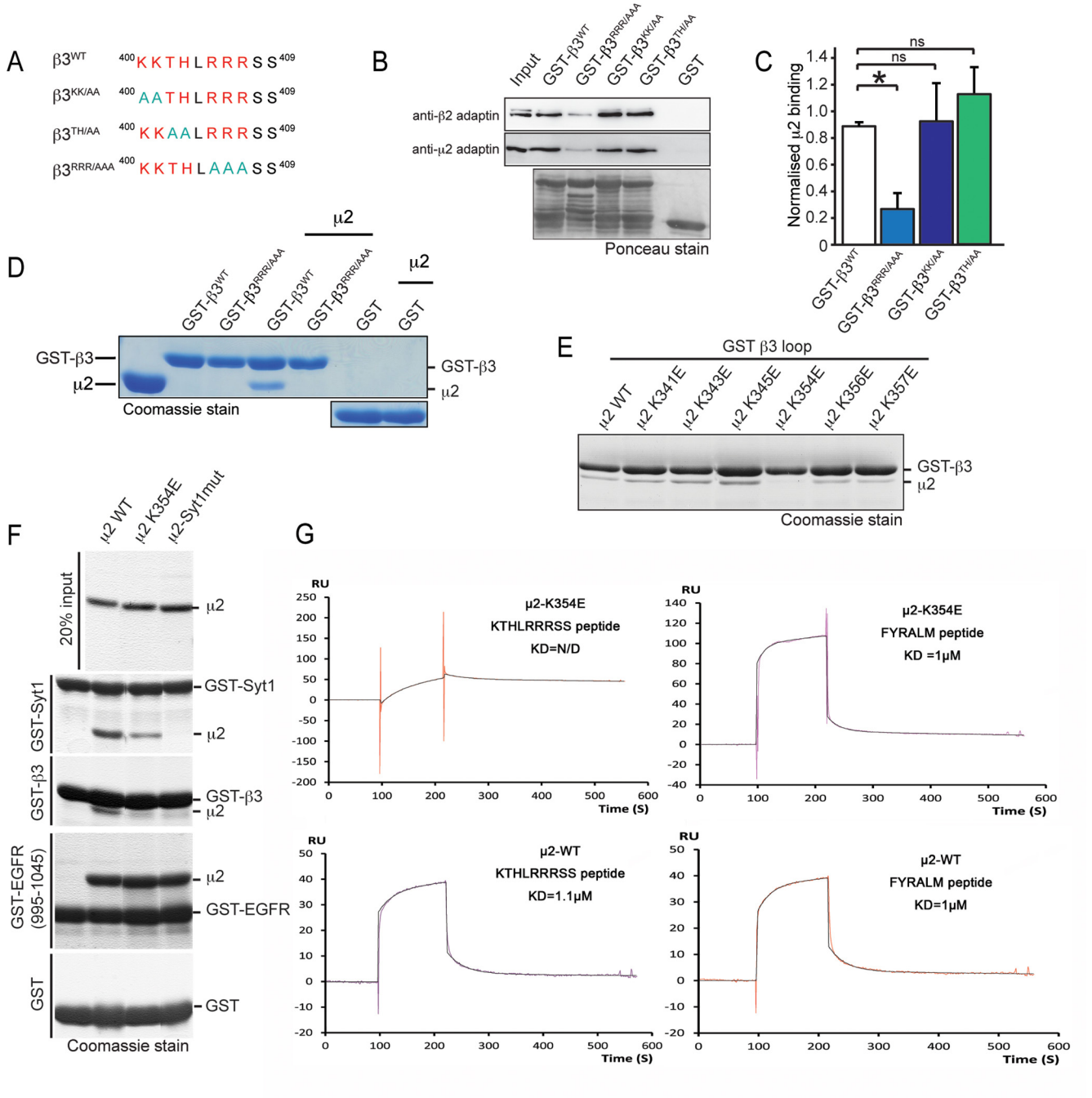

Figure 2. Molecular determinants of the AP2/GABA$_A$R β3-subunit interaction. ***A***, Sequence of the basic amino acid stretch of the β3-subunit ICD showing the basic amino acids (red) and their sequential mutation to alanine residues (blue). ***B–D***, The arginine residues in the β3 subunit mediate its interaction with AP2. ***B***, Pull-down experiments in rat brain lysate with WT, KK, TH, and RRR β3 ICD mutant GST fusion proteins. Protein complexes were analyzed by SDS-PAGE and Western blotting with antibodies to the β2 and μ2 subunits of the AP2 complex. ***C***, Quantification of AP2 binding by densitometry showed a large 3.6-fold decrease in binding to GST–β3$^{RRR/AAA}$ ($n = 3$, $^*p < 0.05$), whereas there was no significant decrease in binding to the KK or TH mutants. ***D***, *In vitro* pull-down experiments with the β3-subunit mutant GST fusion proteins with and without His–μ2. Protein complexes were analyzed by SDS-PAGE and stained with Coomassie blue. ***E***, *In vitro* pull-down experiments with the β3-subunit GST fusion protein and WT His–μ2 and lysine mutants of His–μ2. Protein complexes were analyzed by SDS-PAGE and stained with Coomassie blue. ***F***, ***G***, The β3-subunit ICD and EGFR bind distinct regions of μ2–AP2. ***F***, *In vitro* pull-down experiments with Syt-1–GST, β3–GST, EGFR–GST, and GST as a control, and WT His–μ2, K354E–His–μ2, and Syt-1mut–His-μ2 (which is incapable of binding to Syt-1). Protein complexes were analyzed by SDS-PAGE and stained with Coomassie blue. ***G***, SPR sensograms showing binding of WT and mutant His–μ2 to β3-basic patch and FYRALM peptides, demonstrating that the K354E mutation in μ2 reduces its affinity for the β3 peptide but not for the EGFR peptide. K_D values are given in the figure. N/D, No interaction was detectable. RU, Response units.

(Fig. 2*B*). Direct binding of μ2–AP2 to the RRR motif was further confirmed by *in vitro* pull-down assays using GST–β3^{WT} and GST–β3$^{RRR/AAA}$ with bacterially expressed His–μ2 (Fig. 2*D*), which also showed a large decrease in the direct binding of His–μ2–AP2 to GST–β3$^{RRR/AAA}$ compared with GST–β3^{WT}.

The amino acid residues within the μ2 subunit of AP2 responsible for the interaction with the β3 ICD are not known. Atypical basic-patch motif containing membrane cargo (such as Syt-1) are known to interact with subdomain B of μ2–AP2 (residues 283–394). In the case of Syt-1, key residues within this region of μ2–

AP2 are important for the binding of Syt-1 (Haucke et al., 2000). We therefore tested the binding of His–μ2, containing a series of lysine (K) residue mutations, to the GST–β3 fusion protein by performing pull-down assays with variants of μ2 containing key K residues in subdomain B mutated (Fig. 2*E*). These experiments revealed that mutation of K354 to glutamate (E) within His–μ2 is sufficient to abolish its binding to the β3 ICD (Fig. 2*E*), suggesting that this residue is critical for β3-subunit—AP2 complex formation. To support this finding, additional pull-down experiments were performed with wild-type His–μ2, mutant K354E–His–μ2 (its binding to β3 abolished), and, as an additional control, His–μ2–Syt-1mut (with key additional subdomain B residues mutated preventing its binding to Syt-1: K343A, Y344A, K345E, E348A, K354E, and K356E) and GST–β3 (Fig. 2*F*). This revealed that the K354E–His–μ2 and His–μ2–Syt-1mut mutants exhibited significantly reduced binding to GST–β3 (and with GST–Syt-1, as a control) but could still interact with GST fusion protein of the C-terminal tail of the EGF receptor (EGFR) (residues 995–1045), which associates with a different region of μ2–AP2 via tyrosine-based endocytic motifs (Owen and Evans, 1998) (Fig. 2*F*). The key role of His–μ2 for β3 binding was further supported by SPR experiments that compared the binding affinities of His–μ2 and His–μ2–K354E to a ^{401}KTHLRRRSS^{409} peptide (the β3 ICD basic patch motif) or FYRALM peptide (an EGFR-derived tyrosine-based endocytic motif). Both endocytic sorting motif peptides bind to wild-type His–μ2 with a similar K_D value of $\sim$1 μM. In agreement with the GST pull-downs (Fig. 2*F*), the SPR experiments showed that the μ2 K354E mutation selectively prevents binding to the basic atypical motif within the β3 ICD but not to the tyrosine motif within the EGFR peptide (Fig. 2*G*). These observations lead to the conclusion that the $GABA_A$R β3-subunit binds μ2–AP2 via a minimal ^{405}RRR^{407} motif, to a domain within μ2–AP2, which is distinct from the C-terminal pocket region of μ2–AP2 that binds tyrosine-based motifs such as those within EGFR.

AP2–β3-subunit interactions stabilize $GABA_A$Rs at EZs but not synapses

Having identified a key AP2-binding site in $GABA_A$R β3 subunits, we proceeded to investigate the role of β3-subunit-mediated AP2 binding for regulating the dynamics of $GABA_A$Rs at EZs in hippocampal neuronal dendrites. As a prelude to investigating the role of AP2 adaptor interactions in stabilizing $GABA_A$Rs to EZs, we initially characterized the membrane dynamics of β3-subunit-containing receptors in dendrites with respect to EZs. To test this, we visualized single $GABA_A$R-containing myc-epitope-tagged wild-type $GABA_A$R ($^{myc}\beta3^{WT}$) subunits, using QD tracking (Muir et al., 2010), a well-established method for following the behavior of single receptors in the surface membrane (Triller and Choquet, 2008). To examine $GABA_A$R mobility using this method in relation to regions of endocytosis in the neuronal plasma membrane, we simultaneously labeled EZs by cotransfecting neurons with YFP-tagged clathrin light chain, which has been used previously to label these subdomains in dendrites (Blanpied et al., 2002; Petrini et al., 2009). Single myc-tagged $GABA_A$Rs were labeled using a low concentration of rabbit anti-myc antibody in conjunction with an anti-rabbit secondary coupled to 605 nm QDs. Single QD-labeled $^{myc}\beta3^{WT}$-containing $GABA_A$Rs could be observed to rapidly diffuse into and out of EZs (Fig. 3*A*,*B*) and were less mobile when at EZs compared with outside these subdomains (median $D_{in} = 0.008\ \mu m^2 s^{-1}$, median $D_{out} = 0.020\ \mu m^2 s^{-1}$).

We then used QD tracking of mutant $GABA_A$Rs to directly investigate the role of interactions with the AP2 complex on receptor lateral mobility at EZs. Strikingly, the lateral mobility of mutant $^{myc}\beta3^{RRR/AAA}$-containing $GABA_A$Rs inside EZs was 3.3-fold higher compared with wild-type receptors at EZs [$^{myc}\beta3^{RRR/AAA}$ median $D_{in} = 0.027$, $^{myc}\beta3^{WT}$ median $D_{in} = 0.008\ \mu m^2 s^{-1}$, $^{***}p = 2.2 \times 10^{-16}$, Kolmogorov-Smirnov (K–S) test (Fig. 3*C*); $^{myc}\beta3^{RRR/AAA}$ median $D_{out} = 0.032$, $^{myc}\beta3^{WT}$ median $D_{out} = 0.020\ \mu m^2 s^{-1}$, $^{***}p = 2.2 \times 10^{-16}$ (Fig. 3*D*)]. In agreement with mutant receptors being less stable at EZs, mutation of the three arginine residues caused a significant decrease in the mean time spent by $GABA_A$Rs at EZs ($^{myc}\beta3^{WT}$, 0.81 $\pm$ 0.18 s, $n = 12$ cells; $^{myc}\beta3^{RRR/AAA}$, 0.42 $\pm$ 0.03 s, $n = 11$ cells; $^{*}p = 0.05$), suggesting that mutation of the RRR motif disrupts the interaction required to stabilize $GABA_A$Rs at dendritic EZs before their endocytosis.

We also investigated the mobility and residency time of individual $^{myc}\beta3^{RRR/AAA}$- containing $GABA_A$Rs at inhibitory synapses. Inhibitory presynaptic terminals were live labeled using an antibody to the luminal domain of the GABA transporter VGAT, coupled to the fluorophore Oyster-488 (Martens et al., 2008), which we confirmed were GAD-6 positive (Fig. 3*E*,*F*). QD–$GABA_A$R trajectories were analyzed inside and outside of synaptic locations (as determined by VGAT puncta). Both $^{myc}\beta3^{WT}$- and $^{myc}\beta3^{RRR/AAA}$-containing $GABA_A$Rs were slower at synapses compared with their extrasynaptic counterparts. Inside synapses, $^{myc}\beta3^{WT}$ and $^{myc}\beta3^{RRR/AAA}$ lateral mobility was very similar ($^{myc}\beta3^{WT}$ median $D = 0.00882\ \mu m^2 s^{-1}$; $^{myc}\beta3^{RRR/AAA}$ median $D = 0.00887\ \mu m^2 s^{-1}$; $p = 0.77$, K–S test), suggesting that the RRR motif is not important in stabilizing receptors at synapses. Outside synapses, $^{myc}\beta3^{RRR/AAA}$ receptors were 1.3-fold more mobile than $^{myc}\beta3^{WT}$ receptors ($^{myc}\beta3^{WT}$ median $D = 0.0137\ \mu m^2 s^{-1}$; $^{myc}\beta3^{RRR/AAA}$ median $D = 0.0180\ \mu m^2 s^{-1}$; $^{***}p = 2 \times 10^{-16}$, K–S test). This is likely attributable to the fact that EZs (at which mutant receptors are faster than wild-type receptors) are found extrasynaptically. In agreement with the finding that wild-type and mutant receptor mobilities are similar at synapses, we found no difference in the mean time spent by these receptors at synapses ($^{myc}\beta3^{WT}$, 1.29 $\pm$ 0.22 s, $n = 14$ cells; $^{myc}\beta3^{RRR/AAA}$, 1.36 $\pm$ 0.33 s, $n = 11$ cells; $p = 0.70$). Together, these experiments show the RRR AP2-binding motif in the β3 subunit is important in regulating $GABA_A$R stabilization at EZs but does not affect the stabilization of individual receptors at inhibitory synapses.

Mutation of three arginine residues within the β-subunit ICD impairs $GABA_A$R endocytosis

We predicted that, because $^{myc}\beta3^{RRR/AAA}$ mutant-containing $GABA_A$Rs are less efficiently recruited to EZs and spend less time at these sites, the endocytosis of these mutant receptors would be disrupted. To test this, we performed antibody feeding experiments with COS-7 cells expressing $\alpha1^{myc}\beta3^{WT}$ or $\alpha1^{myc}\beta3^{RRR/AAA}$ $GABA_A$Rs and GFP (Fig. 4*A*). Quantification of $GABA_A$R internalization by normalization of the internalized receptor area to the total cell area (as given by GFP fluorescence, arbitrary units) revealed a significant decrease in $\alpha1^{myc}\beta3^{RRR/AAA}$ receptor endocytosis (0.78 $\pm$ 0.07) compared with $\alpha1^{myc}\beta3^{WT}$ receptors (2.92 $\pm$ 0.50, $n = 3$, $^{*}p < 0.05$). Similar antibody feeding assays were performed on COS-7 cells cotransfected with other β3-subunit mutants analyzed for AP2 binding in Figure 1 ($^{myc}\beta3^{7A}$, $^{myc}\beta3^{ILL/AAA}$, $^{myc}\beta3^{7A+ILL/AAA}$, and $^{myc}\beta3^{\Delta395-414}$). COS-7 cells expressing the $\alpha1^{myc}\beta3^{7A}$ (0.47 $\pm$ 0.22), $\alpha1^{myc}\beta3^{7A+ILL}$ (0.68 $\pm$ 0.11), and $\alpha1^{myc}\beta3^{\Delta395-414}$ (0.56 $\pm$ 0.21) mutant $GABA_A$Rs all displayed significantly reduced endocytosis levels compared with $\alpha1^{myc}\beta3^{WT}$ and $\alpha1^{myc}\beta3^{ILL/AAA}$ receptors ($\alpha1^{myc}\beta3$WT, 1.5 $\pm$ 0.3; $\alpha1^{myc}\beta3^{ILL/AAA}$, 1.47 $\pm$ 0.3; $n = 3$, $^{*}p < 0.05$; Fig. 4*B*).

In similar experiments with COS-7 cells cotransfected with RFP–rab5, an early endosomal marker (Fig. 4*C*), quantification

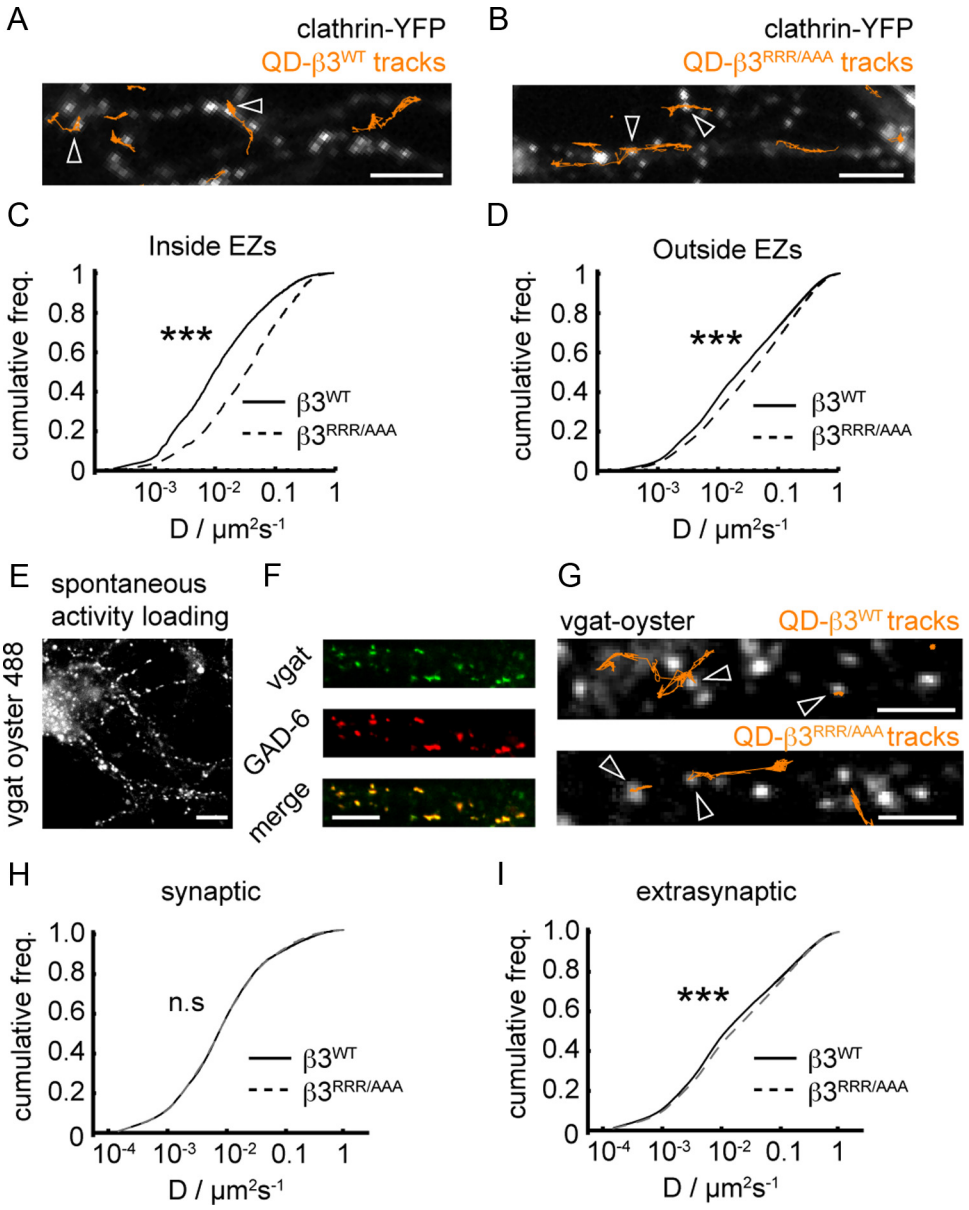

Figure 3. Interactions with AP2 stabilize $GABA_A$Rs at EZs. ***A***, Trajectories of QD-tagged $^{myc}\beta3^{WT}$ subunits (orange) shown overlaid onto the location of clathrin–YFP-labeled EZs (in white). Scale bar, 5 μm; imaging duration, 23.5 s. Arrows indicate examples in which QD-tagged $GABA_A$Rs are within EZs. ***B***, As in *A* but for QD-tagged $^{myc}\beta3^{RRR/AAA}$ subunits. ***C***, Cumulative frequency plots of the instantaneous diffusion coefficients for QD-tagged $^{myc}\beta3^{WT}$ (solid line) and $^{myc}\beta3^{RRR/AAA}$ (dashed line) subunits inside EZs as marked by clathrin–YFP. $GABA_A$Rs containing $^{myc}\beta3^{RRR/AAA}$ subunits are 3.3-fold more mobile than $^{myc}\beta3^{WT}$ within EZs ($^{***}p = 2.2 \times 10^{-16}$, K–S test; $^{myc}\beta3^{WT}$ $n_{in} = 13{,}785$; $^{myc}\beta3^{RRR/AAA}$ $n_{in} = 10{,}836$). ***D***, As in *C*, for $^{myc}\beta3^{WT}$ (solid line) and $^{myc}\beta3^{RRR/AAA}$ (dashed line) subunits outside EZs. $GABA_A$Rs containing $\beta3$ subunits with RRR/AAA mutation are 1.63-fold more mobile than WT outside EZs ($^{***}p = 2.2 \times 10^{-16}$, K–S test; $^{myc}\beta3^{WT}$ $n_{out} = 150{,}884$; $^{myc}\beta3^{RRR/AAA}$ $n_{out} = 200{,}986$). ***E***, Section of example neuron showing GABAergic terminals loaded with VGAT-Oyster 488. ***F***, Dendrite of neuron with GABAergic terminals loaded with VGAT-Oyster 488 and stained with GAD-6 antibody. ***G***, QD-tagged $GABA_A$R trajectories (orange) shown overlaid on VGAT loading (inhibitory synapses) for $^{myc}\beta3^{WT}$ receptors (top) and $^{myc}\beta3^{RRR/AAA}$ mutant receptors (bottom). Arrows point to trajectories in synaptic areas. ***H***, Cumulative frequency plots of instantaneous diffusion coefficients for $^{myc}\beta3^{WT}$ and $^{myc}\beta3^{RRR/AAA}$ receptors at synapses (positions given by VGAT loading). Mobilities at inhibitory synapses are not significantly different ($p = 0.77$, K–S test; $^{myc}\beta3^{WT}$ $n_{in} = 10{,}341$; $^{myc}\beta3^{RRR/AAA}$ $n_{in} = 8250$). ***I***, As in *H* but for extrasynaptic regions. $^{myc}\beta3^{RRR/AAA}$ receptors are 1.3-fold more mobile extrasynaptically ($p = 2 \times 10^{-16}$, K–S test; $^{myc}\beta3^{WT}$ $n_{out} = 127{,}452$; $^{myc}\beta3^{RRR/AAA}$ $n_{out} = 91{,}211$).

of the colocalization of internalized receptors with rab5-labeled compartments revealed that RRR mutant $GABA_A$Rs displayed significantly decreased colocalization with rab5 compared with WT receptors ($^{myc}\beta3^{WT}$, 24.0 ± 0.4%; $^{myc}\beta3^{RRR/AAA}$, 12.5 ± 1.4%; $n = 4$, $^{**}p < 0.01$; Fig. 4*C*). This was also the case with the other mutant receptors, revealing decreased colocalization with rab5-labeled compartments for the $\alpha1^{myc}\beta3^{7A}$, $\alpha1^{myc}\beta3^{ILL/AAA}$, and $\alpha1^{myc}\beta3^{\Delta395-414}$ receptors [$\alpha1^{myc}\beta3^{7A}$, 13.17 ± 0.55% ($^{*}p < 0.05$); $\alpha1^{myc}\beta3^{7A+ILL/AAA}$, 20.02 ± 3.21% ($^{*}p < 0.05$); and $\alpha1^{myc}\beta3^{\Delta395-414}$, 9.48 ± 1.50% ($^{**}p < 0.01$)] compared with their wild-type counterparts (30.42 ± 1.53%; Fig. 4*D*). However, $\alpha1^{myc}\beta3^{ILL/AAA}$ mutant receptors displayed almost identical levels of colocalization with rab5 as wild-type receptors (30.68 ± 2.98%, $p = 0.7$), suggesting that the dileucine motif does not play a significant role in the endocytosis of $\alpha1\beta3$-containing receptors to the early endosome compartment in COS-7 cells.

To also test whether a similar mechanism of $GABA_A$R endocytosis occurs in neurons, we transfected neurons with $^{myc}\beta3^{WT}$ or $^{myc}\beta3^{RRR/AAA}$ constructs, which assemble with endogenous subunits in neurons (data not shown), and performed a similar

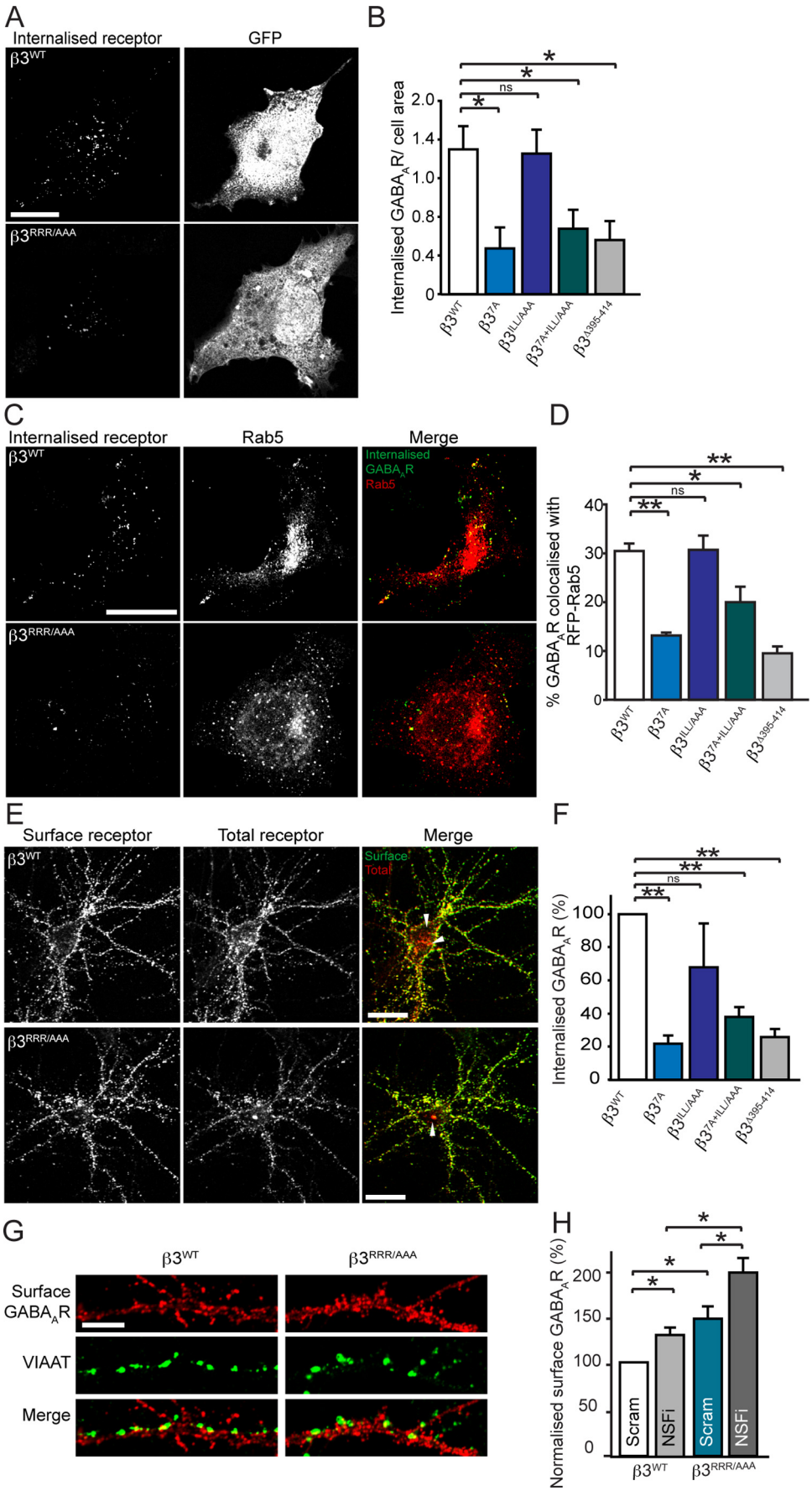

Figure 4. Mutation of the RRR motif impairs GABA$_A$R endocytosis and causes their surface accumulation. ***A***, COS-7 cells coexpressing GABA$_A$Rs ($\alpha1^{myc}\beta3$ or $\alpha1^{myc}\beta3^{RRR/AAA}$) and GFP were live labeled with anti-myc antibody and placed at 37°C for 30 min to allow internalization of receptors. Remaining surface antibody was stripped away and cells were fixed, (*Figure legend continues.*)

antibody feeding protocol. Surface receptors were labeled with myc antibody, left to internalize at 37°C for 30 min, and then fixed and blocked under nonpermeabilizing conditions. Surface receptors were labeled with Alexa Fluor 488-conjugated secondary antibody (green; surface), and, after permeabilization, all myc-tagged receptors were labeled with Alexa Fluor-594-conjugated secondary antibody (red; total), enabling the internalized receptors to be quantified (Fig. 4*E*). Quantification of the internalized pool of receptors (red fluorescence) showed a 72.0 ± 5.0% decrease in the endocytosis of the mutant $^{myc}\beta3^{RRR/AAA}$-containing $GABA_A$Rs compared with wild-type receptors ($n = 3$, $^{**}p < 0.01$; Fig. 4*E*), suggesting that the RRR motif is essential for $GABA_A$R internalization in neurons. Neurons expressing $^{myc}\beta3^{7A}$, $^{myc}\beta3^{7A+ILL/AAA}$, and $^{myc}\beta3^{\Delta395-414}$ mutants also exhibited a similar decrease in percentage endocytosis ($^{myc}\beta3^{7A}$, 78.14 ± 4.70%; $^{myc}\beta3^{7A+ILL/AAA}$, 62.14 ± 6.06%; $^{myc}\beta3^{\Delta395-414}$, 74.24 ± 5.00% decrease in the extent of receptor endocytosis compared with $^{myc}\beta3^{WT}$ control levels; $n = 3$, $^{**}p < 0.01$; Fig. 4*F*, images not shown). In contrast, the $^{myc}\beta3^{ILL/AAA}$ mutant subunits were not significantly altered in their endocytosis compared with $^{myc}\beta3^{WT}$-subunit-containing receptors (32.03 ± 26.23% decrease, $p = 0.3$). Therefore, in both COS-7 cells and neurons, the mutation of the RRR motif within the β3 subunit to alanine residues disrupts the endocytosis of $GABA_A$Rs.

In agreement with these findings, whole-cell ELISAs (Bedford et al., 2001; Mielke and Wang, 2005) in cortical neurons expressing either $^{myc}\beta3^{WT}$ or $^{myc}\beta3^{RRR/AAA}$ constructs revealed that neurons transfected with the $^{myc}\beta3^{RRR/AAA}$ mutant displayed a significant 61.6 ± 8.0% increase in surface $GABA_A$Rs compared with neurons expressing $^{myc}\beta3^{WT}$ receptors ($n = 3$, $^{**}p < 0.01$). To support these data, we then used confocal microscopy to quantify the total area of $GABA_A$R clusters in neurons expressing either the $^{myc}\beta3^{WT}$ or $^{myc}\beta3^{RRR/AAA}$ constructs. Similarly, the total area of $GABA_A$R clusters in neurons expressing the $^{myc}\beta3^{RRR/AAA}$ mutant was 68.0 ± 28.2% greater than that of neurons expressing the $^{myc}\beta3^{WT}$ construct ($n = 3$, $^{**}p < 0.01$; Fig. 4*G*). Therefore, mutation of residues (^{405}RRR^{407}) within the β3 subunit leads to steady-state accumulation of $GABA_A$Rs at the cell surface and at synapses as a result of a decrease in clathrin-dependent endocytosis.

The observed alterations in surface levels and lateral mobility of $^{myc}\beta3^{RRR/AAA}$ mutant $GABA_A$Rs could also possibly be attributable to the effects of NSF, an ATPase that binds to a potentially overlapping region of the β3 ICD as AP2 (Goto et al., 2005) and is implicated in $GABA_A$R trafficking (Chou et al., 2010). To confirm that NSF function was not involved in the observed increased surface expression of $^{myc}\beta3^{RRR/AAA}$ mutant $GABA_A$Rs, we treated COS-7 cells expressing $\alpha1^{myc}\beta3^{WT}$ or $\alpha1^{myc}\beta3^{RRR/AAA}$ $GABA_A$Rs with an NSF inhibitory peptide (NSFi; fused to the TAT sequence), shown previously to increase $GABA_A$R surface expression, or a scrambled control peptide (Morrell et al., 2005; Chou et al., 2010). ELISA experiments were then used to verify surface $GABA_A$R levels. The NSFi peptide treatment caused a 35.3 ± 7.2% increase in surface $\alpha1^{myc}\beta3^{WT}$ $GABA_A$Rs compared with scrambled peptide treatment (Fig. 4*H*). A similar effect on NSF inhibition was also observed for surface $\alpha1^{myc}\beta3^{RRR/AAA}$ $GABA_A$Rs [47.7 ± 14.08% increase in surface $\alpha1^{myc}\beta3^{RRR/AAA}$ $GABA_A$Rs on NSFi treatment compared with scrambled peptide treatment ($n = 4$, $^{*}p < 0.05$)]. These results confirm that the $^{myc}\beta3^{RRR/AAA}$ mutant still undergoes regulatory control by NSF-dependent trafficking mechanisms and that the observed increase in surface $^{myc}\beta3^{RRR/AAA}$ mutant expression is not attributable to altered regulation by NSF via this motif. NSF-dependent interactions were also unlikely to play a role in the observed alterations in surface $GABA_A$R lateral mobility of mutant $\beta3^{RRR/AAA}$ receptors, because QD-imaging experiments revealed that blocking NSF activity had very little effect on the lateral mobility of $GABA_A$Rs at the plasma membrane (data not shown). We therefore conclude that the effects of the RRR/AAA mutation on $GABA_A$Rs at the neuronal cell surface are attributable to the specific disruption of the β3/AP2 binding site.

β3-subunit AP2 interactions are critical for $GABA_A$R depletion from synapses during ischemic insult

An imbalance between excitatory and inhibitory synaptic transmission is thought to contribute to excitotoxicity and neuronal cell death during ischemic insult. Several studies have reported a decrease in surface and synaptic $GABA_A$R expression during ischemia, suggesting an increase in receptor endocytosis (Schwartz-Bloom and Sah, 2001; Mielke and Wang, 2005; Zhan et al., 2006; Kelley et al., 2008; Arancibia-Cárcamo et al., 2009; Liu et al., 2010), but whether this is via an AP2-dependent pathway remains unclear.

To monitor the role of AP2 interactions in $GABA_A$R trafficking, we used a super-ecliptic pHluorin (pH-sensitive GFP) N-terminally tagged γ2-subunit construct ($^{SEP}\gamma2$), cotransfected with β3 subunits to visualize surface and synaptic $GABA_A$R clusters under normal and ischemic conditions using live-cell imaging techniques. This cotransfection also enabled us to study effects of mutations within both γ2 and β3 subunits. Hippocampal neurons were cotransfected with $^{SEP}\gamma2$, $\alpha1$, and either the $^{myc}\beta3^{WT}$ or the AP2-binding-deficient $^{myc}\beta3^{RRR/AAA}$ or $^{myc}\beta3^{7A}$ constructs. Quantification of the cotransfection efficiency of these DNAs revealed that 93.3 ± 3.3 and 96.6 ± 3.3% of $^{SEP}\gamma2$-transfected cells were cotransfected with $^{myc}\beta3^{WT}$ or $^{myc}\beta3^{RRR/AAA}$, respectively, indicating a high and similar level of cotransfection for these experiments (data not shown). Similar transfection effi-

←

Figure 4. (*Figure legend continued*) permeabilized, and labeled with secondary antibody. Quantification of $GABA_A$R endocytosis by normalization of the internalized receptor area to the total cell area (as given by GFP fluorescence) showed decreased internalization of $^{myc}\beta3^{RRR/AAA}$ receptors compared with $^{myc}\beta3^{WT}$ receptors ($^{myc}\beta3^{WT}$, 2.92 ± 0.50; $^{myc}\beta3^{RRR/AAA}$, 0.78 ± 0.07; $n = 3$, $^{*}p < 0.05$). ***B***, Summary of data from similar antibody feeding experiments with $^{myc}\beta3^{WT}$, $^{myc}\beta3^{7A}$, $^{myc}\beta3^{ILL/AAA}$, $^{myc}\beta3^{7A+ILL/AAA}$, and $^{myc}\beta3^{\Delta395-414}$ containing $GABA_A$Rs. ***C***, Antibody feeding experiments in COS-7 cells coexpressing $GABA_A$Rs ($\alpha1^{myc}\beta3^{WT}$ or $\alpha1^{myc}\beta3^{RRR/AAA}$) and RFP–rab5. Receptor internalization was measured as the percentage colocalization of receptors with rab5 and showed a 50% decrease in internalization of $\alpha1^{myc}\beta3^{RRR/AAA}$ mutant $GABA_A$Rs compared with wild-type receptors ($^{myc}\beta3^{WT}$, 24.0 ± 0.4%; $^{myc}\beta3^{RRR/AAA}$, 12.5 ± 1.4%; $^{**}p < 0.01$, $n = 4$). ***D***, Summary of data from similar antibody feeding experiments with $^{myc}\beta3^{WT}$, $^{myc}\beta3^{7A}$, $^{myc}\beta3^{ILL/AAA}$, $^{myc}\beta3^{7A+ILL/AAA}$, and $^{myc}\beta3^{\Delta395-414}$ containing $GABA_A$Rs. ***E***, DIV 12–14 neurons expressing $^{myc}\beta3^{WT}$ or $^{myc}\beta3^{RRR/AAA}$ subunits were treated with an antibody feeding protocol. Fluorescence of internalized receptors was represented as a fraction of the total fluorescence of the cell and normalized to values for $^{myc}\beta3^{WT}$-transfected cells. Red fluorescence indicates internalized receptors. The internalization of $^{myc}\beta3^{RRR/AAA}$-containing receptors was reduced to 28.0 ± 5.0% compared with $^{myc}\beta3^{WT}$ receptors ($n = 3$, $^{**}p < 0.01$). Arrows point to internalized receptor population (red). ***F***, Quantification of similar antibody feeding experiments in neurons expressing $^{myc}\beta3^{7A}$, $^{myc}\beta3^{ILL/AAA}$, $^{myc}\beta3^{7A+ILL/AAA}$, and $^{myc}\beta3^{\Delta395-414}$ receptors. Scale bars, 20 μm. ***G***, Cluster counting analysis of 25 μm dendritic segments of neurons expressing $^{myc}\beta3^{WT}$ or $^{myc}\beta3^{RRR/AAA}$ revealed a 68.0 ± 23.2% ($n = 3$, $^{**}p < 0.01$) increase in total surface receptor cluster area. Scale bar, 5 μm. ***H***, ELISA experiments were performed with COS-7-expressing $\alpha1^{myc}\beta3^{WT}$ or $\alpha1^{myc}\beta3^{RRR/AAA}$ $GABA_A$R subunits that were treated with either an NSFi or a scrambled control peptide (Scram). The NSFi peptide caused a 35.3 ± 7.2% increase in surface $\alpha1^{myc}\beta3^{WT}$ $GABA_A$Rs and a 47.7 ± 14.08% increase in surface $\alpha1^{myc}\beta3^{RRR/AAA}$ $GABA_A$Rs ($n = 4$, $^{*}p < 0.05$).

ciencies were also obtained for the $^{myc}\beta3^{7A}$ construct (data not shown).

We imaged $^{SEP}\gamma2$ and $^{myc}\beta3^{WT}$ cotransfected 12–15 DIV hippocampal neurons under control conditions or under conditions of OGD, an *in vitro* experimental model used to mimic cerebral ischemia (Kelley et al., 2008; Arancibia-Cárcamo et al., 2009). The fluorescence of individual $^{SEP}\gamma2$ clusters in neuronal dendrites was imaged over a 30 min time period. Analysis of $^{SEP}\gamma2$ cluster fluorescence in neurons cotransfected with $^{myc}\beta3^{WT}$ showed that the $^{SEP}\gamma2$ cluster fluorescence remained stable under control conditions (Fig. 5*A*,*B*). However, during the OGD treatment, there was a significant 21.3 ± 4.0% reduction in surface cluster fluorescence over time compared with the control ($n = 12$, $^{**}p < 0.01$; Fig. 5*A*,*B*). Using this approach, we then investigated whether this downmodulation was dependent on β3-subunit/AP2 interactions. In contrast to the $^{myc}\beta3^{WT}/^{SEP}\gamma2$-containing receptors, the surface $^{SEP}\gamma2$ cluster fluorescence was not reduced on OGD treatment in neurons cotransfected with either the $^{myc}\beta3^{7A}$ or $^{myc}\beta3^{RRR/AAA}$ mutant subunits with impaired endocytic ability ($p = 0.71$ and $p = 0.36$, respectively; Fig. 5*C–F*,*I*).

A $GABA_AR$ AP2-binding domain (YECL) in the γ2 subunit also exists (Kittler et al., 2008). In contrast, mutating the YECL AP2-binding domain in the γ2 subunit (to AECL) led to significant decrease in $GABA_AR$ cluster intensity under OGD conditions ($^{*}p < 0.05$; Fig. 5*G*,*J*). However, in neurons cotransfected with $^{myc}\beta3^{RRR/AAA}$ and $^{SEP}\gamma2^{AECL}$, $GABA_ARs$ were stable at the cell surface over the OGD time course ($p = 0.77$; Fig. 5*H*,*J*). Thus, the RRR motif within the β3 subunit is more important for control of AP2-mediated $GABA_AR$ internalization during OGD insult than the YECL motif on the γ2 subunit. Therefore, these experiments show that the interaction of the β3 subunit with AP2 plays a key role in the loss of synaptic $GABA_ARs$ observed during ischemia. Furthermore, these data reveal that specific targeting of this $GABA_AR$ RRR AP2-binding motif could provide resistance for $GABA_ARs$ against their accelerated endocytosis and removal from synaptic sites induced by ischemic insult.

Blockade of the β3/AP2 interaction reduces neuronal cell death during ischemic insult

We have revealed that preventing the interaction of $GABA_AR$ β3 subunit and AP2 can maintain surface $GABA_AR$ clusters during OGD. To investigate the functional relevance of this finding, we used a peptide overlapping the AP2 binding region in the β3 subunit to compete the β3/AP2 interaction in hippocampal neurons (β3 peptide). The β3 peptide and a control peptide (to a region of the β3 ICD distinct from the AP2 binding site) were transduced into 12–15 DIV hippocampal neurons for 1 h before OGD insult using a membrane-permeable carrier peptide (Twelvetrees et al., 2010). Delayed neuronal death was analyzed 24 h later using PI and DAPI staining, and the number of PI-positive nuclei were counted and the cell viability determined (Fig. 6*A*,*B*). OGD treatment of neurons transduced with the control peptide caused a 30.5 ± 1.6% decrease in cell viability ($n = 3$, $^{***}p < 0.001$) compared with neurons pretreated with the β3 peptide that exhibited an insignificant 6.4 ± 1.4% reduction in cell viability ($n = 3$, $p = 0.09$). These data show that specifically blocking the β3/AP2 interaction in neurons can prevent OGD-induced delayed cell death, strongly suggesting that $GABA_AR$ endocytosis via the RRR motif is important in mediating this process.

Discussion

Regulated trafficking of postsynaptic neurotransmitter receptors is essential for determining the strength of synaptic transmission and for ensuring the correct balance of excitation and inhibition of neuronal circuits (Groc and Choquet, 2006; Arancibia-Cárcamo and Kittler, 2009). Tightly controlled clathrin-dependent endocytosis of surface $GABA_ARs$ has been specifically shown to control synaptic efficacy in neurons, providing a fast mechanism to modulate synaptic strength and therefore synaptic inhibition (Kittler et al., 2000, 2008). Reduced inhibition attributable to alterations in $GABA_AR$ trafficking can also contribute to disrupted information processing and to the detrimental excitotoxicity thought to exacerbate neuronal cell death observed in conditions such as stroke and epilepsy (Smith and Kittler, 2010). In this study, we have investigated the internalization mechanisms of β3-subunit-containing $GABA_ARs$ under normal and pathological conditions. We have identified a specific RRR motif (^{405}RRR^{407}) within the β3-subunit ICD that is essential for the endocytosis of $GABA_ARs$. We show that these residues mediate the direct interaction with μ2–AP2, although K354 within μ2–AP2 is also critical for this interaction. Mutation of the β3-subunit RRR motif reduces recruitment of $GABA_ARs$ to EZs and impairs their endocytosis, leading to their steady-state accumulation at the neuronal cell surface and at synapses. We also show that downmodulation of $GABA_ARs$ from dendritic clusters during OGD treatment (to simulate ischemia) is dependent on an AP2-dependent pathway for cell-surface removal of receptors. Moreover, blockade of this pathway can reduce the delayed neuronal death observed during ischemic insult.

We focused our study on the internalization of $GABA_ARs$ containing the β3 subunit because of its high expression in the hippocampus and cortex and its presence in a large proportion of $GABA_AR$ subtypes found in these regions (Laurie et al., 1992; Wisden et al., 1992). To identify the molecular determinants of $GABA_AR$ internalization, we first identified the region of the β3-subunit ICD that mediated the interaction with the clathrin-adaptor protein AP2. This revealed a 20 aa stretch that harbored a seven residue atypical basic patch motif that, when mutated to alanine, prevented the binding of AP2 to the $GABA_AR$ β3-subunit ICD. Within this binding motif, additional mapping identified three arginine residues (^{405}RRR^{407}) that are essential for the interaction with μ2–AP2 and receptor internalization via an AP2- and clathrin-dependent mechanism. Because μ2–AP2 binds to $GABA_AR$ subunits β1–β3 and the RRR motif is conserved across all three β subunits, it suggests that these residues might be an internalization signal for all β-subunit-containing $GABA_ARs$. An arginine residue (R845) was also shown to be critical for AMPA receptor GluR2 subunit binding to AP2 (Lee et al., 2002; Kastning et al., 2007). Atypical basic patch motifs of both AMPA and $GABA_ARs$ bind to the same region of μ2–AP2, subdomain B (Kastning et al., 2007; and this study), pointing to a similar clathrin-mediated internalization mechanism for both types of postsynaptic neurotransmitter receptors. In contrast, we did not find that a putative dileucine motif within the β3 subunit [as suggested for the β2 subunit (Herring et al., 2003)] was required for endocytosis or AP2 binding, suggesting that this motif is not a primary determinant of β3-subunit-mediated $GABA_AR$ internalization. Interestingly, the β3-subunit RRR motif is located adjacent to a phosphorylation site, Ser^{408}/Ser^{409}, which acts as a key site for $GABA_AR$ phosphomodulation by kinases (Brandon et al., 2002) and phosphatases (Jovanovic et al., 2004; Terunuma et al., 2008). Phosphorylation at this site has been shown to impair $GABA_AR$ endocytosis by preventing the interaction of the β3-subunit with AP2 (Kittler et al., 2005; Jacob et al., 2009). The addition of phosphate groups to Ser^{408}/Ser^{409} would create a large negative charge that may disrupt the local charge interac-

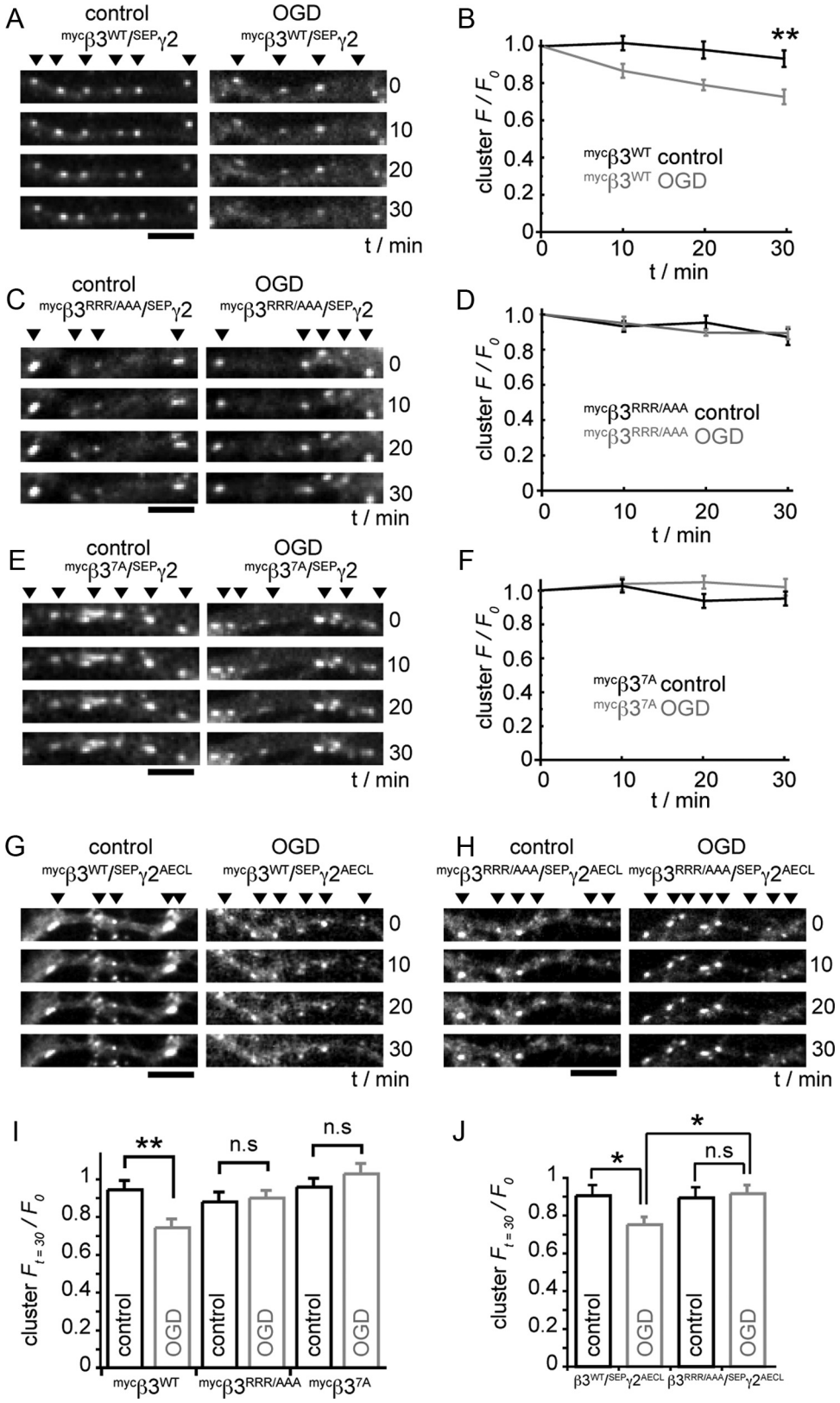

Figure 5. GABA$_A$Rs that are unable to bind AP2 are not removed from synapses during OGD. ***A***, ***C***, ***E***, Twelve to 15 DIV hippocampal neurons expressing $^{SEP}\gamma2$ and $^{myc}\beta3^{WT}$, $^{myc}\beta3^{RRR/AAA}$, or $^{myc}\beta3^{7A}$ were imaged over time under control or OGD conditions. Twenty micrometer sections of dendrite are shown. ***B***, ***D***, ***F***, Fluorescent clusters in dendrites were monitored for loss of GFP fluorescence over time and normalized to $t = 0$. ***B***, $^{myc}\beta3^{WT}$ control $t = 30$ min, 0.94 ± 0.04 ($n = 12$); $^{myc}\beta3^{WT}$ OGD $t = 30$, 0.74 ± 0.04 ($n = 12$, $^{**}p < 0.01$). ***D***, $^{myc}\beta3^{RRR/AAA}$ control $t = 30$ min, 0.87 ± 0.05 ($n = 7$); $^{myc}\beta3^{RRR/AAA}$ OGD $t = 30$, 0.89 ± 0.03 ($n = 6$, $p = 0.71$, nonsignificant). ***F***, $^{myc}\beta3^{7A}$ control $t = 30$ min, 0.95 ± 0.04 ($n = 4$); $^{myc}\beta3^{7A}$ OGD $t = 30$, 1.02 ± 0.05 ($n = 6$, $p = 0.36$, nonsignificant). Arrows point to $^{SEP}\gamma2$ clusters. ***G***, ***H***, Twelve to 15 DIV hippocampal neurons expressing $^{SEP}\gamma2^{AECL}$ with either $^{myc}\beta3^{WT}$ or $^{myc}\beta3^{RRR/AAA}$ subunits were imaged over time under OGD conditions. ***G***, $^{myc}\beta3^{WT}/^{SEP}\gamma2^{AECL}$ control, 0.90 ± 0.03, $n = 5$; OGD, 0.75 ± 0.05, $n = 5$; $^{*}p < 0.05$. ***H***, $^{myc}\beta3^{RRR/AAA}/^{SEP}\gamma2^{AECL}$ control, 0.89 ± 0.04, $n = 5$; OGD, 0.91 ± 0.05, $n = 8$; $p = 0.77$. Twenty micrometer sections of dendrite are shown. ***I***, ***J***, Bar graphs summarizing the fluorescent cluster analysis. Scale bars, 5 μm.

tions provided by the arginine residue cluster, thereby disrupting the AP2 binding site.

We have used QD tracking to measure the lateral mobility of $GABA_A$Rs within EZs, specialized clathrin-rich regions along the dendritic plasma membrane, which mediate clathrin-dependent endocytosis (Blanpied et al., 2002). We found that QD-labeled $GABA_A$Rs could be reversibly recruited to these clathrin-rich structures in which they displayed a reduced lateral mobility compared with receptors outside the EZ, suggesting that the receptors are being confined to these subdomains, before their endocytosis. This is similar to the confined behavior of $GABA_A$Rs observed at the inhibitory postsynaptic site, with similar diffusion coefficient values for the mobility of the receptors previously recorded at the synapse to those observed at EZs (Bannai et al., 2009; Muir et al., 2010). This suggests that both inhibitory postsynaptic sites and EZs are specialized dendritic subdomains that share similar $GABA_A$R confinement mechanisms via reversible interactions with submembranous synaptic or EZ proteins, such as gephyrin and AP2, respectively. In agreement with this, mutation of the RRR motif to alanine impaired the recruitment of $GABA_A$Rs to EZs, as shown by the 3.3-fold increase in lateral mobility of non-AP2-binding mutant $GABA_A$Rs at clathrin-coated pits compared with their wild-type counterparts. This increase in lateral mobility was accompanied by a significantly decreased residency time for the mutant receptors at EZs and a reduced likelihood of mutant receptors being endocytosed. Mutation of the β3-subunit AP2-binding motif did not alter the mobility or residency time of individual $GABA_A$Rs at synaptic sites but did increase the steady-state levels of surface and synaptic receptors as a result of diminished receptor endocytosis. These results clearly demonstrate the key role of direct interactions of $GABA_A$R ICDs with AP2 for recruiting and confining $GABA_A$Rs at endocytic sites. This allows the trapping of mobile receptor populations at these membrane compartments within the plasma membrane to enable $GABA_A$Rs to either mediate phasic inhibition at the synapse or undergo receptor endocytosis at the EZ.

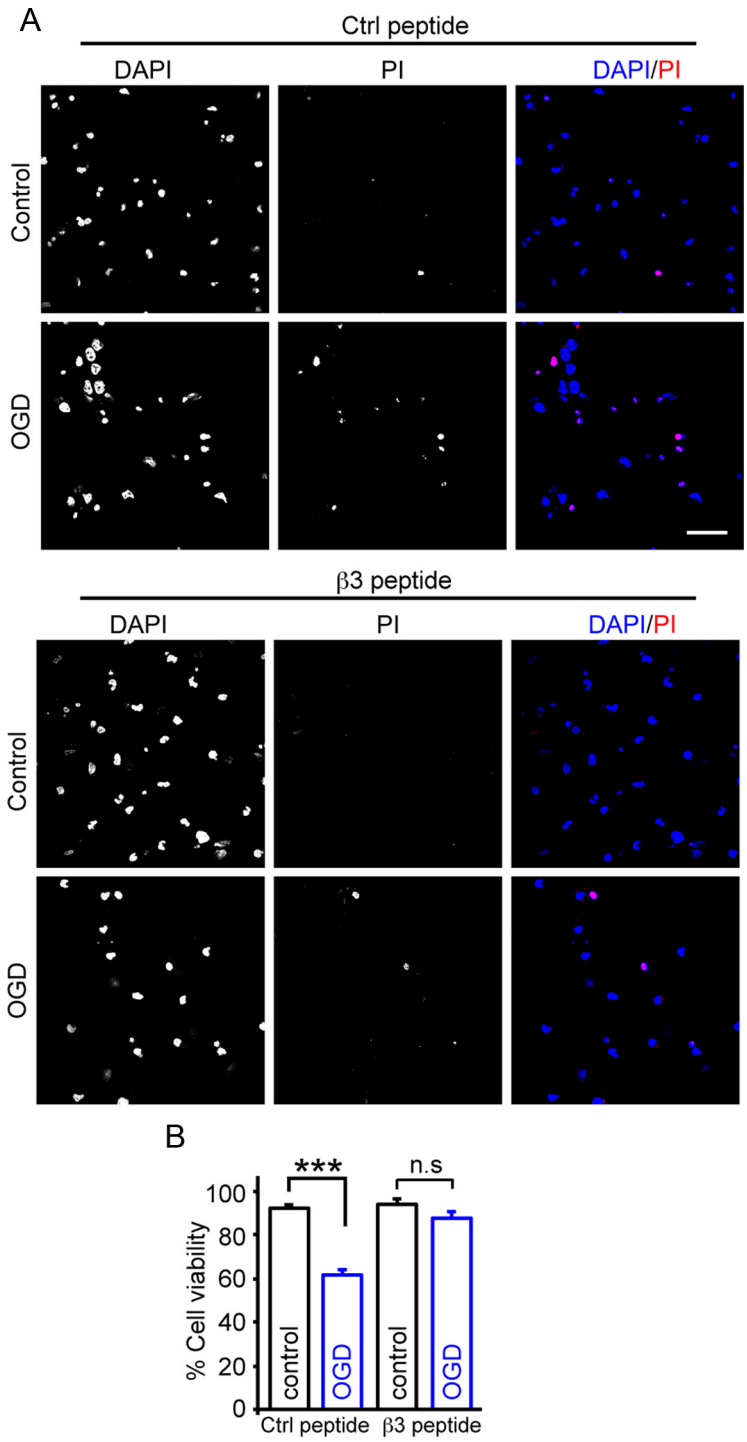

Figure 6. Blockade of $GABA_A$R endocytosis reduces OGD-induced delayed cell death. Twelve to 15 DIV hippocampal neurons were transduced with control or β3 peptides for 1 h before a 40 min OGD treatment. Twenty-four hours later, neurons were stained with PI and DAPI, and the PI-positive nuclei were counted. ***A***, Representative confocal images of control and β3 peptide transduced neurons under control and OGD conditions. Scale bar, 40 μm. ***B***, Bar graph summarizing the pooled data ($n = 3$, $^{***}p < 0.001$).

During cerebral ischemia, overexcitation as a result of excessive glutamate release contributes to excitotoxicity and cell death in susceptible neuronal populations (Lipton, 1999; Lo et al., 2003). Research into therapeutics to treat ischemia has focused primarily on the glutamatergic system and the reduction of excess glutamatergic signaling during ischemic insult, but these have not proven to be clinically effective (Schwartz-Bloom and Sah, 2001). GABAergic transmission and $GABA_A$R endocytosis are also significantly altered in ischemia, which may contribute to disinhibition and pathological excitability states. Because glutamatergic neurotransmission is counterbalanced by the GABAergic system, modulation of GABA metabolism and $GABA_A$R function may be alternative targets of therapeutic intervention for ischemia. An *in vitro* model of cerebral ischemia, OGD, has been shown to modulate $GABA_A$R trafficking, reducing surface expression of receptors (Mielke and Wang, 2005; Liu et al., 2010)

and increasing ubiquitin-dependent lysosomal receptor degradation (Arancibia-Cárcamo et al., 2009). Previous studies using hypertonic sucrose treatment or dynamin inhibitors have suggested that pathological $GABA_AR$ endocytosis in OGD or status epilepticus is attributable to clathrin-dependent endocytosis (Goodkin et al., 2005; Mielke and Wang, 2005). However, hypertonicity has multiple cellular effects (Rosenmund and Stevens, 1996; Carroll et al., 1999), and dynamin inhibitors may block other (e.g., caveolar) endocytosis pathways (Nabi and Le, 2003; Doherty and McMahon, 2009). By imaging super-ecliptic pHluorin-tagged $GABA_ARs$, we show a decrease in synaptic $GABA_AR$ clusters during OGD treatment of hippocampal neurons for 30 min, which is consistent with other studies (Mielke and Wang, 2005; Arancibia-Cárcamo et al., 2009; Liu et al., 2010). Using the β3-subunit RRR motif mutant, we then directly tested the pathway of pathological $GABA_AR$ endocytosis during OGD and showed that acute loss of synaptic $GABA_ARs$ during OGD is mediated by an AP2 and clathrin-dependent internalization pathway. Furthermore, blocking this internalization pathway with a competing β3 peptide can reduce delayed cell death after OGD insult, demonstrating the physiological relevance of this mechanism in neuronal function.

We also find that the tyrosine motif within the γ2 subunit has little effect on endocytosis of $GABA_ARs$ during OGD, suggesting that the β3-subunit RRR motif is the primary determinant of internalization during simulated ischemic insult. This is probably attributable to the different binding affinities of the subunits for AP2 and their regulation by different kinase families (Kittler et al., 2005, 2008), allowing multiple signaling pathways to converge at these receptor ICDs, to enable the fine-tuning of endocytosis modulation in response to a variety of extracellular signals.

In summary, we have identified a triple arginine motif that mediates direct binding of the $GABA_AR$ β3 subunit to the clathrin adaptor protein AP2. Mutation of this motif impaired receptor recruitment to clathrin-coated pits, significantly reduced receptor endocytosis, and caused an accumulation of surface $GABA_ARs$ in neurons. This AP2 pathway is likely to play a key role in regulating synaptic receptor number during inhibitory synaptic plasticity. In ischemia, synaptic $GABA_ARs$ are also depleted by this AP2/clathrin-dependent pathway. This internalization pathway might therefore also be targeted therapeutically to maintain surface $GABA_AR$ populations and synaptic inhibition during pathological insults such as epilepsy and ischemic neuronal death.

References

Arancibia-Cárcamo IL, Kittler JT (2009) Regulation of GABA(A) receptor membrane trafficking and synaptic localization. Pharmacol Ther 123:17–31.

Arancibia-Cárcamo IL, Yuen EY, Muir J, Lumb MJ, Michels G, Saliba RS, Smart TG, Yan Z, Kittler JT, Moss SJ (2009) Ubiquitin-dependent lysosomal targeting of GABA(A) receptors regulates neuronal inhibition. Proc Natl Acad Sci U S A 106:17552–17557.

Bannai H, Lévi S, Schweizer C, Inoue T, Launey T, Racine V, Sibarita JB, Mikoshiba K, Triller A (2009) Activity-dependent tuning of inhibitory neurotransmission based on GABAAR diffusion dynamics. Neuron 62:670–682.

Bedford FK, Kittler JT, Muller E, Thomas P, Uren JM, Merlo D, Wisden W, Triller A, Smart TG, Moss SJ (2001) GABA(A) receptor cell surface number and subunit stability are regulated by the ubiquitin-like protein Plic-1. Nat Neurosci 4:908–916.

Blanpied TA, Scott DB, Ehlers MD (2002) Dynamics and regulation of clathrin coats at specialized endocytic zones of dendrites and spines. Neuron 36:435–449.

Bradley CA, Taghibiglou C, Collingridge GL, Wang YT (2008) Mechanisms involved in the reduction of GABAA receptor alpha1-subunit expression caused by the epilepsy mutation A322D in the trafficking-competent receptor. J Biol Chem 283:22043–22050.

Brandon NJ, Jovanovic JN, Smart TG, Moss SJ (2002) Receptor for activated C kinase-1 facilitates protein kinase C-dependent phosphorylation and functional modulation of $GABA_A$ receptors with the activation of G-protein-coupled receptors. J Neurosci 22:6353–6361.

Carroll RC, Beattie EC, Xia H, Lüscher C, Altschuler Y, Nicoll RA, Malenka RC, von Zastrow M (1999) Dynamin-dependent endocytosis of ionotropic glutamate receptors. Proc Natl Acad Sci U S A 96:14112–14117.

Chen C, Zhuang X (2008) Epsin 1 is a cargo-specific adaptor for the clathrin-mediated endocytosis of the influenza virus. Proc Natl Acad Sci U S A 105:11790–11795.

Chen G, Kittler JT, Moss SJ, Yan Z (2006) Dopamine D_3 receptors regulate GABAA receptor function through a phospho-dependent endocytosis mechanism in nucleus accumbens. J Neurosci 26:2513–2521.

Chou WH, Wang D, McMahon T, Qi ZH, Song M, Zhang C, Shokat KM, Messing RO (2010) $GABA_A$ receptor trafficking is regulated by protein kinase Cε and the *N*-ethylmaleimide-sensitive factor. J Neurosci 30:13955–13965.

Collins BM, McCoy AJ, Kent HM, Evans PR, Owen DJ (2002) Molecular architecture and functional model of the endocytic AP2 complex. Cell 109:523–535.

Diviani D, Lattion AL, Abuin L, Staub O, Cotecchia S (2003) The adaptor complex 2 directly interacts with the alpha 1b-adrenergic receptor and plays a role in receptor endocytosis. J Biol Chem 278:19331–19340.

Dixon RM, Mellor JR, Hanley JG (2009) PICK1-mediated glutamate receptor subunit 2 (GluR2) trafficking contributes to cell death in oxygen/glucose-deprived hippocampal neurons. J Biol Chem 284:14230–14235.

Doherty GJ, McMahon HT (2009) Mechanisms of endocytosis. Annu Rev Biochem 78:857–902.

Dumoulin A, Rostaing P, Bedet C, Lévi S, Isambert MF, Henry JP, Triller A, Gasnier B (1999) Presence of the vesicular inhibitory amino acid transporter in GABAergic and glycinergic synaptic terminal boutons. J Cell Sci 112:811–823.

Goodkin HP, Yeh JL, Kapur J (2005) Status epilepticus increases the intracellular accumulation of $GABA_A$ receptors. J Neurosci 25:5511–5520.

Goto H, Terunuma M, Kanematsu T, Misumi Y, Moss SJ, Hirata M (2005) Direct interaction of *N*-ethylmaleimide-sensitive factor with GABA(A) receptor beta subunits. Mol Cell Neurosci 30:197–206.

Groc L, Choquet D (2006) AMPA and NMDA glutamate receptor trafficking: multiple roads for reaching and leaving the synapse. Cell Tissue Res 326:423–438.

Hanley JG, Henley JM (2005) PICK1 is a calcium-sensor for NMDA-induced AMPA receptor trafficking. EMBO J 24:3266–3278.

Haucke V, Wenk MR, Chapman ER, Farsad K, De Camilli P (2000) Dual interaction of synaptotagmin with mu2- and alpha-adaptin facilitates clathrin-coated pit nucleation. EMBO J 19:6011–6019.

Herring D, Huang R, Singh M, Robinson LC, Dillon GH, Leidenheimer NJ (2003) Constitutive GABAA receptor endocytosis is dynamin-mediated and dependent on a dileucine AP2 adaptin-binding motif within the beta 2 subunit of the receptor. J Biol Chem 278:24046–24052.

Jacob TC, Wan Q, Vithlani M, Saliba RS, Succol F, Pangalos MN, Moss SJ (2009) GABA(A) receptor membrane trafficking regulates spine maturity. Proc Natl Acad Sci U S A 106:12500–12505.

Jovanovic JN, Thomas P, Kittler JT, Smart TG, Moss SJ (2004) Brain-derived neurotrophic factor modulates fast synaptic inhibition by regulating $GABA_A$ receptor phosphorylation, activity, and cell-surface stability. J Neurosci 24:522–530.

Kastning K, Kukhtina V, Kittler JT, Chen G, Pechstein A, Enders S, Lee SH, Sheng M, Yan Z, Haucke V (2007) Molecular determinants for the interaction between AMPA receptors and the clathrin adaptor complex AP-2. Proc Natl Acad Sci U S A 104:2991–2996.

Kelley MH, Taguchi N, Ardeshiri A, Kuroiwa M, Hurn PD, Traystman RJ, Herson PS (2008) Ischemic insult to cerebellar Purkinje cells causes diminished GABAA receptor function and allopregnanolone neuroprotection is associated with GABAA receptor stabilization. J Neurochem 107:668–678.

Kittler JT, Delmas P, Jovanovic JN, Brown DA, Smart TG, Moss SJ (2000)

Constitutive endocytosis of GABAA receptors by an association with the adaptin AP2 complex modulates inhibitory synaptic currents in hippocampal neurons. J Neurosci 20:7972–7977.

Kittler JT, Thomas P, Tretter V, Bogdanov YD, Haucke V, Smart TG, Moss SJ (2004) Huntingtin-associated protein 1 regulates inhibitory synaptic transmission by modulating gamma-aminobutyric acid type A receptor membrane trafficking. Proc Natl Acad Sci U S A 101:12736–12741.

Kittler JT, Chen G, Honing S, Bogdanov Y, McAinsh K, Arancibia-Carcamo IL, Jovanovic JN, Pangalos MN, Haucke V, Yan Z, Moss SJ (2005) Phospho-dependent binding of the clathrin AP2 adaptor complex to GABAA receptors regulates the efficacy of inhibitory synaptic transmission. Proc Natl Acad Sci U S A 102:14871–14876.

Kittler JT, Chen G, Kukhtina V, Vahedi-Faridi A, Gu Z, Tretter V, Smith KR, McAinsh K, Arancibia-Carcamo IL, Saenger W, Haucke V, Yan Z, Moss SJ (2008) Regulation of synaptic inhibition by phospho-dependent binding of the AP2 complex to a YECL motif in the GABAA receptor gamma2 subunit. Proc Natl Acad Sci U S A 105:3616–3621.

Kurotani T, Yamada K, Yoshimura Y, Crair MC, Komatsu Y (2008) State-dependent bidirectional modification of somatic inhibition in neocortical pyramidal cells. Neuron 57:905–916.

Laurie DJ, Wisden W, Seeburg PH (1992) The distribution of thirteen $GABA_A$ receptor subunit mRNAs in the rat brain. III. Embryonic and postnatal development. J Neurosci 12:4151–4172.

Lee SH, Liu L, Wang YT, Sheng M (2002) Clathrin adaptor AP2 and NSF interact with overlapping sites of GluR2 and play distinct roles in AMPA receptor trafficking and hippocampal LTD. Neuron 36:661–674.

Lipton P (1999) Ischemic cell death in brain neurons. Physiol Rev 79: 1431–1568.

Liu B, Li L, Zhang Q, Chang N, Wang D, Shan Y, Li L, Wang H, Feng H, Zhang L, Brann DW, Wan Q (2010) Preservation of GABAA receptor function by PTEN inhibition protects against neuronal death in ischemic stroke. Stroke 41:1018–1026.

Lo EH, Dalkara T, Moskowitz MA (2003) Mechanisms, challenges and opportunities in stroke. Nat Rev Neurosci 4:399–415.

Macaskill AF, Rinholm JE, Twelvetrees AE, Arancibia-Carcamo IL, Muir J, Fransson A, Aspenstrom P, Attwell D, Kittler JT (2009) Miro1 is a calcium sensor for glutamate receptor-dependent localization of mitochondria at synapses. Neuron 61:541–555.

Martens H, Weston MC, Boulland JL, Grønborg M, Grosche J, Kacza J, Hoffmann A, Matteoli M, Takamori S, Harkany T, Chaudhry FA, Rosenmund C, Erck C, Jahn R, Härtig W (2008) Unique luminal localization of VGAT-C terminus allows for selective labeling of active cortical GABAergic synapses. J Neurosci 28:13125–13131.

Mielke JG, Wang YT (2005) Insulin exerts neuroprotection by counteracting the decrease in cell-surface GABA receptors following oxygen-glucose deprivation in cultured cortical neurons. J Neurochem 92:103–113.

Morrell CN, Matsushita K, Lowenstein CJ (2005) A novel inhibitor of *N*-ethylmaleimide-sensitive factor decreases leukocyte trafficking and peritonitis. J Pharmacol Exp Ther 314:155–161.

Muir J, Arancibia-Carcamo IL, MacAskill AF, Smith KR, Griffin LD, Kittler JT (2010) NMDA receptors regulate GABAA receptor lateral mobility and clustering at inhibitory synapses through serine 327 on the gamma2 subunit. Proc Natl Acad Sci U S A 107:16679–16684.

Nabi IR, Le PU (2003) Caveolae/raft-dependent endocytosis. J Cell Biol 161:673–677.

Naylor DE, Liu H, Wasterlain CG (2005) Trafficking of $GABA_A$ receptors, loss of inhibition, and a mechanism for pharmacoresistance in status epilepticus. J Neurosci 25:7724–7733.

Owen DJ, Evans PR (1998) A structural explanation for the recognition of tyrosine-based endocytotic signals. Science 282:1327–1332.

Petrini EM, Lu J, Cognet L, Lounis B, Ehlers MD, Choquet D (2009) Endocytic trafficking and recycling maintain a pool of mobile surface AMPA receptors required for synaptic potentiation. Neuron 63:92–105.

Rosenmund C, Stevens CF (1996) Definition of the readily releasable pool of vesicles at hippocampal synapses. Neuron 16:1197–1207.

Schwartz-Bloom RD, Sah R (2001) gamma-Aminobutyric acid(A) neurotransmission and cerebral ischemia. J Neurochem 77:353–371.

Scott DB, Michailidis I, Mu Y, Logothetis D, Ehlers MD (2004) Endocytosis and degradative sorting of NMDA receptors by conserved membrane-proximal signals. J Neurosci 24:7096–7109.

Smith KR, Kittler JT (2010) The cell biology of synaptic inhibition in health and disease. Curr Opin Neurobiol 20:550–556.

Smith KR, McAinsh K, Chen G, Arancibia-Carcamo IL, Haucke V, Yan Z, Moss SJ, Kittler JT (2008) Regulation of inhibitory synaptic transmission by a conserved atypical interaction of GABA(A) receptor beta- and gamma-subunits with the clathrin AP2 adaptor. Neuropharmacology 55:844–850.

Smith KR, Oliver PL, Lumb MJ, Arancibia-Carcamo IL, Revilla-Sanchez R, Brandon NJ, Moss SJ, Kittler JT (2010) Identification and characterisation of a Maf1/Macoco protein complex that interacts with GABA(A) receptors in neurons. Mol Cell Neurosci 44:330–341.

Tan HO, Reid CA, Single FN, Davies PJ, Chiu C, Murphy S, Clarke AL, Dibbens L, Krestel H, Mulley JC, Jones MV, Seeburg PH, Sakmann B, Berkovic SF, Sprengel R, Petrou S (2007) Reduced cortical inhibition in a mouse model of familial childhood absence epilepsy. Proc Natl Acad Sci U S A 104:17536–17541.

Terunuma M, Xu J, Vithlani M, Sieghart W, Kittler J, Pangalos M, Haydon PG, Coulter DA, Moss SJ (2008) Deficits in phosphorylation of $GABA_A$ receptors by intimately associated protein kinase C activity underlie compromised synaptic inhibition during status epilepticus. J Neurosci 28: 376–384.

Thévenaz P, Ruttimann UE, Unser M (1998) A pyramid approach to subpixel registration based on intensity. IEEE Trans Image Process 7:27–41.

Tretter V, Revilla-Sanchez R, Houston C, Terunuma M, Havekes R, Florian C, Jurd R, Vithlani M, Michels G, Couve A, Sieghart W, Brandon N, Abel T, Smart TG, Moss SJ (2009) Deficits in spatial memory correlate with modified {gamma}-aminobutyric acid type A receptor tyrosine phosphorylation in the hippocampus. Proc Natl Acad Sci U S A 106: 20039–20044.

Triller A, Choquet D (2008) New concepts in synaptic biology derived from single-molecule imaging. Neuron 59:359–374.

Twelvetrees AE, Yuen EY, Arancibia-Carcamo IL, MacAskill AF, Rostaing P, Lumb MJ, Humbert S, Triller A, Saudou F, Yan Z, Kittler JT (2010) Delivery of GABA(A)Rs to synapses is mediated by HAP1-KIF5 and disrupted by mutant huntingtin. Neuron 65:53–65.

Vonderheit A, Helenius A (2005) Rab7 associates with early endosomes to mediate sorting and transport of Semliki forest virus to late endosomes. PLoS Biol 3:e233.

Wisden W, Laurie DJ, Monyer H, Seeburg PH (1992) The distribution of 13 $GABA_A$ receptor subunit mRNAs in the rat brain. I. Telencephalon, diencephalon, mesencephalon. J Neurosci 12:1040–1062.

Zhan RZ, Nadler JV, Schwartz-Bloom RD (2006) Depressed responses to applied and synaptically-released GABA in CA1 pyramidal cells, but not in CA1 interneurons, after transient forebrain ischemia. J Cereb Blood Flow Metab 26:112–124.